Chapter 2
Experimental Study of Resonant Gamma-Ray Scattering

2.1 Introduction

In 1961, Metzger published an article [1] in which he described an experiment devoted to studying "classic" (without the use of the Mössbauer effect) resonant gamma-ray scattering on ^{57}Fe nuclei. He measured the magnetic moment of the ^{56}Fe nucleus in the first excited state, whose spin–parity is 2^+, by using the internal magnetic field in an annular iron scatterer to perturb the angular distribution (AD) of resonantly scattered gamma rays. There arose the question of whether it is possible to use the Mössbauer scattering of gamma rays for the same purpose of observing corresponding magnetic-field-perturbed ADs of resonantly scattered gamma rays. By that time, it has not yet been clear (at least, to the present author) that, at the first stage of Mössbauer gamma-ray scattering, the nucleus to be excited does not of course experience recoil, nor do violations of the other degrees of freedom occur. Such violations could lead to AD distortions that are difficult to take into account.

In order to obtain an answer to this question, it was necessary to perform an experiment aimed at measuring unperturbed ADs of gamma rays undergoing Mössbauer resonant scattering by nuclei entering into the composition of a substance in which internal magnetic or nonuniform electric fields could not affect ADs. Therefore, a nonmagnetic substance that has a cubic crystal lattice must be the scatterer in such an experiment.

Tungsten in which ^{182}W nuclei must be excited was chosen for this goal. The success of this experiment [2] permitted us to perform a whole series of investigations of both unperturbed and magnetic-field perturbed angular distributions of resonantly scattered gamma rays.

Before presenting these experimental data, it is worthwhile to note that Mössbauer gamma-ray scattering is a particular case where the character of processes of gamma-ray absorption and emission is such that the AD of gamma rays scattered by nuclei of a solid body may remain unperturbed even at average lifetimes of excited nuclei as long as 10^{-9}–10^{-7} s. It is well known that unperturbed angular correlations of

A.V. Davydov, *Advances in Gamma Ray Resonant Scattering and Absorption*,
Springer Tracts in Modern Physics 261, DOI 10.1007/978-3-319-10524-6_2

sequentially emitted photons are usually observed in the case of liquid or gaseous rather than in the case of solid gamma sources. This special feature of Mössbauer scattering is directly related to the fact that, owing to the absence of recoil, the nucleus that absorbed a primary photon remains at its site of the crystal lattice throughout its lifetime in the excited state. At the same time, a nucleus that experienced recoil in the case of "classic" resonant gamma-ray scattering and which moves in the substance of the scatterer undergoes collisions with its atoms, with the result that the quantum numbers of the excited state change. If the scattering nucleus is at a site of the cubic lattice of a nonmagnetic crystal, then, naturally, neither electric-quadrupole nor magnetic-dipole interaction affects this nucleus since there are no internal fields at this site.

2.2 Measurement of the Angular Distribution of 100.1 keV Gamma Rays Resonantly Scattered by ^{182}W Nuclei

The isotope ^{182}W was chosen for the first experiment for the following reasons:

(a) The Mössbauer effect for the 100.1 keV gamma line had already been observed by that time with this isotope in traditional transmission geometry [3–6].
(b) The effect observed in the studies indicated above was rather large at liquid-nitrogen temperature, and this rendered the experiment simpler since there was no need for employing liquid helium.
(c) Metallic tungsten is not a ferromagnet and has a cubic body-centered crystal lattice.
(d) It is convenient to fabricate gamma sources irradiating metallic tantalum with reactor neutrons.

The decay scheme for the parent nuclide ^{182}Ta produced upon neutron absorption by a ^{181}Ta nucleus is shown in Fig. 2.1 [7]. It was proposed to observe the resonant excitation of the 2^+ level of the ^{182}W nucleus at 100.1 keV. In this case, the process of resonant gamma-ray scattering proceeds via the sequence of $0^+ \rightarrow 2^+$ and $2^+ \rightarrow 0^+$ $E2$ transitions. The corresponding AD of resonantly scattered photons is highly anisotropic. Its shape, which is represented by the solid line in Fig. 2.5, is described by the expression

$$W(\theta) = 1 + 0.3571\,P_2(\cos\theta) + 1.1429\,P_4(\cos\theta), \tag{2.1}$$

where $P_2(\cos\theta)$ and $P_4(\cos\theta)$ are Legendre polynomials.

The layout of the experimental setup is shown in Fig. 2.2. A scatterer in the form of a metallic-tungsten plate 0.5 mm thick was arranged in the narrowed part of a Styrofoam container, which may be filled with liquid nitrogen. The thickness of the container walls at the scatterer position was about 15 mm. This was sufficient for preventing the formation of ice at the container walls throughout the measurement time

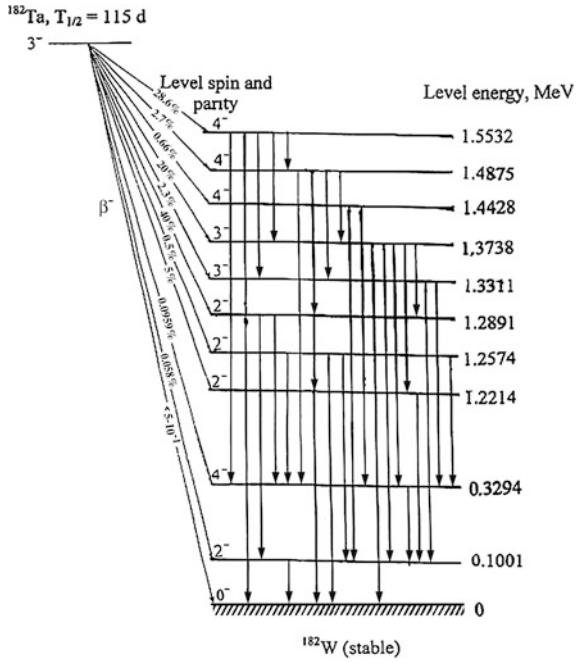

Fig. 2.1 Scheme of β^-decay of ^{182}Ta nucleus and of subsequent gamma transitions in daughter nucleus ^{182}W according to [7]

and for thereby avoiding the additional absorption and scattering of initial and scattered gamma rays in ice. The position of the scatterer in the narrow part of the container permitted minimizing th e contribution of gamma-ray scattering by liquid nitrogen.

A gamma source was made from a tantalum foil 0.1 mm thick in the form of a disk 1 cm in diameter irradiated with thermal reactor neutrons at a flux density of about 2×10^{13} cm^2 s^{-1} for about 100 h. The source was clutched between aluminum plates and fastened to a Plexiglas holder, which was rigidly connected to a moving coil of an electromagnetic vibrator. The lower ends of the aluminum plates were immersed in liquid nitrogen filling the Styrofoam cuvette. The source position was outside liquid nitrogen and was close to its surface, and the source temperature was close to its boiling temperature. The electromagnetic vibrator was an electromagnet with a hollow cylindrical iron yoke inside which there was a magnetizing coil on a iron rod joined to the back wall of the yoke. In the front part of the yoke, there was an annular clearance between it and the central rod, and an alternating-current-carrying coil put on the central rod could oscillate along the magnet axis. The average position of the coil was fixed in the axial direction by two springs. The vibrator, together with the gamma source and the cuvette filled with liquid nitrogen, were closed from the outside by a lead layer of thickness sufficient for reducing the external-radiation level to a permissible value. The initial gamma-ray beam came to the scatterer through a lead collimator. Scattered gamma rays were detected by a

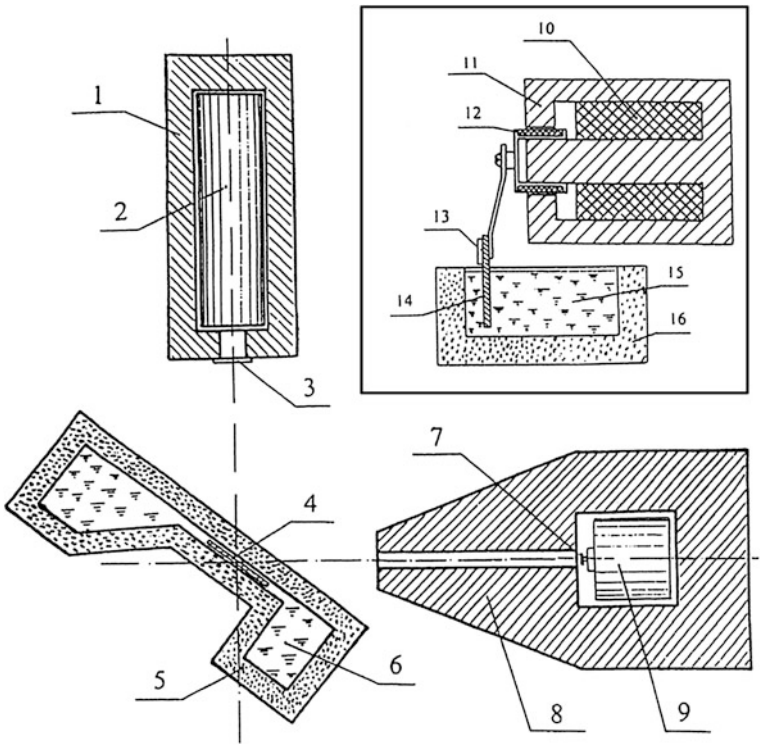

Fig. 2.2 Layout of the setup for measuring unperturbed angular distributions of resonantly scattered gamma rays. The *inset* shows the scheme of fastening of the liquid-nitrogen-cooled gamma source to the movable coil of the electromagnetic vibrator. The following notation is used here: (*1*) protective lead screen of the scintillation detector, (*2*) body of the scintillation detector, (*3*) X-ray filters, (*4*) scatterer, (*5*) Styrofoam container, (*6*) liquid nitrogen, (*7*) gamma source, (*8*) lead "house" with a collimator for the source and vibrator, (*9*) electromagnetic vibrator, (*10*) magnetizing coil of the vibrator, (*11*) iron yoke of the vibrator, (*12*) movable coil of the vibrator, (*13*) gamma source, (*14*) cold finger of the source (the thin aluminum plate pressing the source to the cold finger is not shown), (*15*) liquid nitrogen, and (*16*) Styrofoam cuvette

scintillation counter based on a NaI(Tl) crystal. The detector was placed inside a lead "house" with a window 40 mm in diameter. The collimator, scatterer, and detector were arranged in such a way that, at all scattering angles, the perpendicular to the scatterer plane was the bisector of the angle complementary to the scattering angle. In the case of this geometry and under the condition that the scatterer thickness d was so large that one could treat the scatterer as that which was indefinitely thick for gamma rays of energy interesting to us, the absorption of gamma rays penetrating into the scatterer and going backward after a scattering event was independent of the scattering angle and was therefore immaterial in processing the results of the measurements. Indeed, the number of photons having an energy in the interval between E and $E + dE$ and undergoing scattering at an angle of $\theta = 180^{\circ} - 2\theta'$ in the layer of thickness dx at a depth x is given by (see Fig. 2.3)

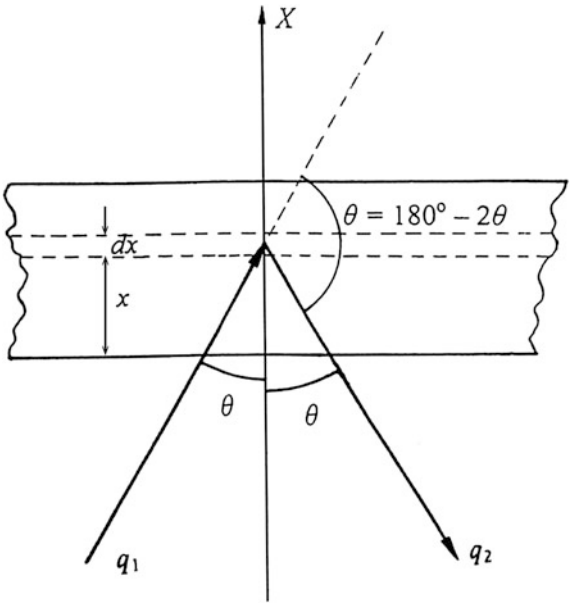

Fig. 2.3 Geometry that was chosen for our experiment aimed at studying gamma-ray scattering and in which the perpendicular to the scatterer plane is the bisector of the angle complementary to the scattering angle θ. Here, q_1 and q_2 are the wave vectors of, respectively, the initial and the scattered photon

$$dN(E,x) = N(E)\, e^{-2v[\sigma_t + 0.5a\sigma_{ra}(E)]\frac{x}{\cos\theta'}} \frac{d\sigma_{rs}(E,\theta)}{d\Omega} av \frac{dxdE}{\cos\theta'}. \tag{2.2}$$

Here, $N(E)dE$ is the number of photons that have an energy between E and $E + dE$ and which are incident to a 1 cm^2 area orthogonal to the gamma-beam axis (we neglect the beam divergence within the scatterer thickness), v is the number of scatterer atoms per 1 cm^3, a is the relative fraction of atoms whose nuclei can resonantly scatter gamma rays, σ_t is the total nonresonant-absorption cross section in the scatterer material for the gamma rays in question, $\sigma_{ra}(E)$ is the energy-dependent total cross section for resonant gamma-ray absorption, $\frac{d\sigma_{rs}(E,\theta)}{d\Omega}$ is the differential cross section for the resonant scattering of gamma rays with energy E at an angle θ into a solid-angle unit, and θ' is half the angle complementary to the scattering angle. The coefficient of 0.5 in front of $a\sigma_{ra}(E)$ in the bracketed expression in the exponent is associated with the fact that the weakening of the gamma-ray intensity because of resonant absorption must be taken into account only before the scattering event. The gamma rays escaping from the scatterer are able to undergo secondary resonant absorption to a smaller degree because of a low probability to be scattered without recoil in primary scattering. the scatterer thickness), v is the number of scatterer atoms per 1 cm^3, a is the relative fraction of atoms whose nuclei can resonantly scatter gamma rays, σ_t is the total nonresonant-absorption cross section in the scatterer material for the gamma rays in question, $\sigma_{ra}(E)$ is the energy-dependent total cross section for resonant gamma-ray absorption, $\frac{d\sigma_{rs}(E,\theta)}{d\Omega}$ is the differential cross section for the resonant scattering of gamma rays with energy E at an angle θ into a solid-angle unit, and θ' is half the

angle complementary to the scattering angle. The coefficient of 0.5 in front of $a\sigma_{ra}(E)$ in the bracketed expression in the exponent is associated with the fact that the weakening of the gamma-ray intensity because of resonant absorption must be taken into account only before the scattering event. The gamma rays escaping from the scatterer are able to undergo secondary resonant absorption to a smaller degree because of a low probability to be scattered without recoil in primary scattering.

Integration of expression (2.2) with respect to x yields

$$dN(E) = N(E)dE\frac{d\sigma_{rs}(E,\theta)}{d\Omega}\frac{a}{2[\sigma_t + 0.5a\sigma_{ra}(E)]}\left\{1 - e^{\frac{-2v[\sigma_t+0.5\sigma_{ra}(E)]d}{\cos\theta'}}\right\}. \quad (2.3)$$

For a rather thick scatterer, the exponential factor is very small, in which case the angular dependence of $dN(E)$ remainsnly in $\frac{d\sigma_{rs}(E,\theta)}{d\Omega}$—that is, it is the true AD of resonantly scattered gamma rays that determines it.

The measurement of the AD of resonantly scattered gamma rays consisted in determining, for each of five chosen scattering angles (90°, 112°, 127°, 141.5°, and 150°), the difference of the number of counts in the scintillation counter for the case where the source was at rest and the case where it performed oscillations of amplitude 0.5 mm at a frequency of 50 Hz. Under these conditions, the maximum velocity of source motion was 15.7 cm/s, which was 150 times as high as the velocity that is necessary for shifting the exciting gamma line with respect to the resonance position by its natural width.

Erbium, gadolinium, and holmium filters were used to reduce the background of tungsten and tantalum X-rays. Because of the smallness of resonant gamma-ray absorption in the scatterer in relation to the total nonresonant absorption, the contribution of Rayleigh scattering was nearly identical in the two measurement modes (source at rest versus moving source). After the subtraction of the background, the remaining difference effect corresponding to the Mössbauer resonant scattering of 100.1 keV gamma rays was 2–4 % (depending on the scattering angle) of the number of counts for the gamma source at rest. A correction associated with the change in the effective average position of the oscillating source in relation to its position at rest was introduced in the numbers of counts corresponding to the resonant-scattering effect. This correction (about 0.5 % of the average number of counts) was determined experimentally from the change in the number of counts in the analyzer channels corresponding to the energy of scattered gamma rays, about 185 keV, upon going over from the source-at-rest to the oscillating-source mode. The background was subtracted simultaneously. Figure 2.4 shows the spectrum of detector pulses that was obtained by means of the channel-by-channel subtraction of the numbers of counts corresponding to the measurement where the vibrator was switched on from their counterparts measured with the gamma source at rest. The peak of the total absorption of resonantly scattered gamma rays with energy 100.1 keV is clearly seen.

The results of the measurements are shown in Fig. 2.5. The scale along the ordinate for the smooth curve representing the unperturbed angular distribution $W(\theta)$ calculated by formula (1.89) was found by the least squares method for one

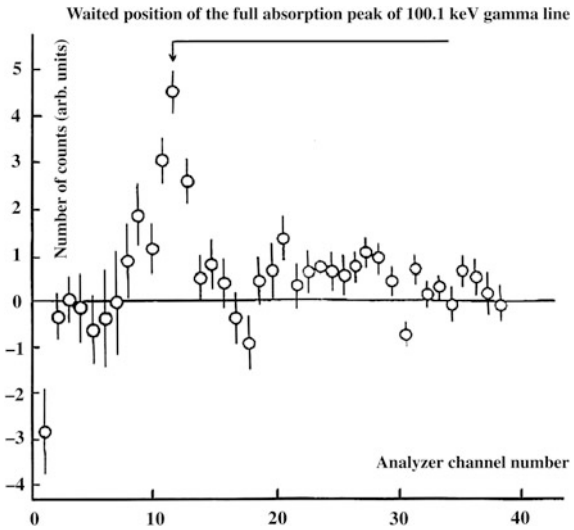

Fig. 2.4 Fragment of the amplitude spectrum of pulses induced in the NaI(Tl) scintillation detector by scattered ^{182}W gamma rays for the expected position of the 100.1 keV gamma line. It was obtained by means of the channel-by-channel subtraction of the number of counts in the mode where the vibrator was switched on from the number of counts in the mode where the vibrator was switched off

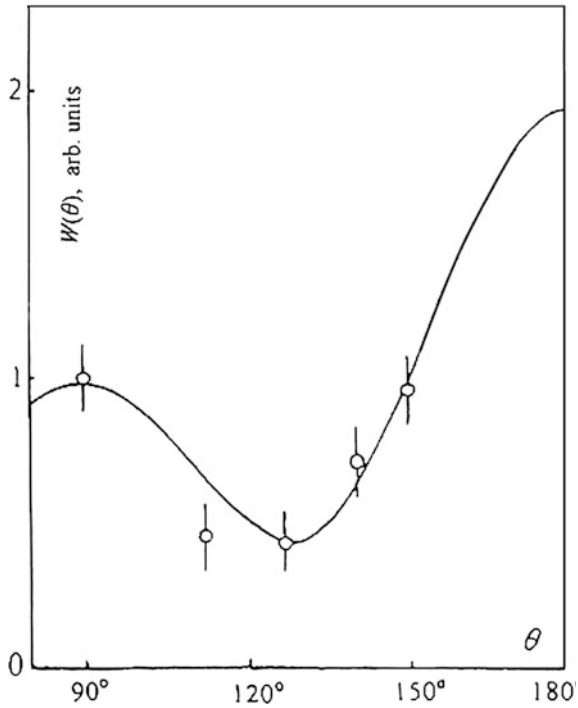

Fig. 2.5 Unperturbed angular distribution of 100.1 keV gamma rays resonantly scattered by ^{182}W nuclei. The *solid curve* represents the theoretical unperturbed-angular distribution matched with experimental data by determining a single parameter (ordinate scale) via a least squares fit

parameter to be determined. For four degrees of freedom that are present in this case, the value of the χ^2 criterion is 2.8. Therefore, the measured AD agrees within the experimental errors with the unperturbed AD calculated for the set of nuclear-level spins being considered. The results of this experiment were published in [2]. This experiment showed that, by using the Mössbauer effect, one could observe, at least in some cases, the unperturbed AD of resonantly scattered gamma rays in the case of comparatively long average lifetimes of nuclear states to be excited. The ADs in question may be highly anisotropic, as in the case of ^{182}W, and this is a favorable circumstance for experiments aimed at measuring the magnetic moments of such nuclei in corresponding excited states.

2.3 Measurement of the Magnetic Moment of the ^{182}W Nucleus in the 2^+ Excited State at 100.1 keV

In order to check the possibility of measuring nuclear magnetic moments by using magnetic-field-perturbed ADs of gamma rays that experienced Mössbauer resonant scattering, we undertaken an experiment aimed at measuring, by this method, the magnetic moment of the ^{182}W nucleus in the already known excited state at 100.1 keV. The layout of the setup used in that experiment is shown in Fig. 2.6. A gamma source in the form of a tantalum-foil disk 0.1 mm thick and 18 mm in diameter was irradiated with thermal reactor neutrons and was soldered after that into a thin-walled brass ampule. The tightly sealed gamma source was placed into a Styrofoam cuvette filled with liquid nitrogen. This cuvette was mounted on the

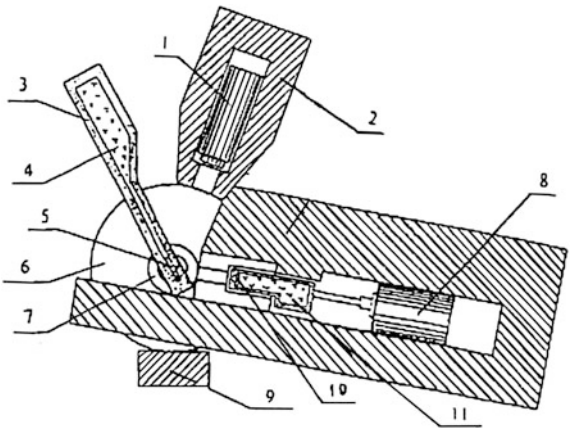

Fig. 2.6 Layout of the setup for measuring the magnetic moment of the ^{182}W nucleus in the excited state at 100.1 keV: (*1*) scintillation detector based on a NaI(Tl) crystal, (*2*) protective lead screens, (*3*) Styrofoam container, (*4*) liquid nitrogen, (*5*) scatterer, (*6*) coil of the electromagnet, (*7*) pole piece of the magnet, (*8*) electromagnetic vibrator, (*9*) yoke of the magnet, (*10*) gamma source, and (*11*) cuvette filled with liquid nitrogen

movable rod of an electromagnetic vibrator and could be driven in oscillatory motion, together with the gamma source, at a frequency of 50 Hz and with an amplitude of 0.5 mm. This was sufficient for substantially violating resonance conditions and for suppressing the resonant-scattering effect to a level below 2 % of the maximum possible level in the case of the source at rest. The vibrator and the cuvette with the gamma source were placed inside a lead "house." A narrow beam of gamma rays from the source came out through a cylindrical collimator. A 0.6-mm-thick scatterer from metallic tungsten of natural isotopic composition was placed in the extension of the Styrofoam container filled with liquid nitrogen. This extension was pushed in the gap between the pole pieces of the electromagnet energized from a stabilized rectifier and used to create, in the scatterer region (19 mm in height and 22 mm in width), a constant magnetic field of strength 13,500 Oe and uniformity not poorer than 2 %. Scattered gamma rays were detected by a NaI(Tl) scintillation detector surrounded by a triple magnetic-shield layer (two iron cylinders 3 mm thick each separated by air gaps and a cylinder 2 mm thick from a Permalloy tape 0.2 mm thick annealed in hydrogen after fabrication. From the outside, the detector was shielded by a lead layer about 5 cm in thickness. The average scattering angle was 109.5°. Effects of resonant gamma-ray scattering were measured for two opposite directions of the magnetic field as the difference of the numbers of counts for the oscillating gamma source and the gamma source at rest under the condition that both the source and the scatterer were at liquid-nitrogen temperature. Corrections for the shift of the source center upon the transition from the state at rest to the state of motion were introduced in the data that we obtained. In order to compare the experimental results with the theoretical expression for the angular distribution, it is convenient to represent these results in the form

$$R' = 2\frac{N^+ - N^-}{N^+ + N^-}, \tag{2.4}$$

where N^+ and N^- are the numbers of counts for the liquid-nitrogen-cooled source and scatterer (numbers of resonantly scattered gamma rays) in the cases of, respectively, the positive and the negative direction of the magnetic field. In expression (1.92), it was necessary to introduce a correction that would take into account the possible influence of the change in the magnetic-field direction on detector operation. This correction, R'', was determined experimentally as a quantity that was analogous to R', but which was measured under conditions where both the scatterer and the gamma source at rest were at room temperature. In that case, there was virtually no resonant scattering.

Therefore, data on the magnetic moment of the ^{182}W nucleus in the excited state at 100.1 keV must be extracted from the quantity $R = R' - R''$, which was measured to be $R = -0.153 \pm 0.031$. The results of that study, which was performed before the appearance of the article quoted in [8], were treated according to the theory that described perturbed angular correlations of sequentially emitted photons without allowance for the ratio of the width Δ of the spectrum of resonantly scattered gamma rays to the natural width Γ of the nuclear level to be excited. We now

reproduce here this line of reasoning and obtain, on its basis, the g-factor value for the ^{182}W nucleus in the excited state of interest and, after that, introduce, in this value, the correction associated with the full theory described in the first chapter, whereupon we compare both values with the results of various experiments.

Expression (2.1) for the angular distribution of resonantly scattered gamma rays can be written in a simpler form; that is,

$$W(\theta) = 1 - 3\cos^2\theta + 4\cos^4\theta. \tag{2.5}$$

Denoting by $N^+(\theta)$ [$N^-(\theta)$] the number of photons recorded by the detector and resonantly scattered at an angle θ in the case of a positive (negative) direction of the magnetic field and assuming that the measurement time was much longer than the mean lifetime of the nucleus in the excited state, we obtain

$$N^{\pm}(\theta) = \int_0^{\infty} e^{-t/\tau} W(\theta \pm \Omega t) dt, \tag{2.6}$$

where τ is the mean lifetime of nuclei in the excited state (it is related to the natural width Γ of this state by the equation $\tau\Gamma = \hbar$) and Ω is the Larmor frequency of nuclear-spin precession in the magnetic field.

Substituting Eq (2.5) into Eq (2.6) and performing integration, one obtains

$$N^{\pm}(\theta) = \tau\left[1 + 0,5\cos 2\theta \frac{1}{1+4\Omega^2\tau^2} \mp 0,5\sin 2\theta \frac{2\Omega\tau}{1+4\Omega^2\tau^2} + 0,5\cos 4\theta \frac{1}{1+16\Omega^2\tau^2} \mp 0,5\sin 4\theta \frac{4\Omega\tau}{1+16\Omega^2\tau^2}\right]. \tag{2.7}$$

From here, it follows that R can be represented in the form

$$R = 2\frac{N^+(\theta) - N^-(\theta)}{N^+(\theta) + N^-(\theta)} = -\frac{4\Omega\tau\left[\frac{\sin 2\theta}{1+4\Omega^2\tau^2} + \frac{2\sin 4\theta}{1+16\Omega^2\tau^2}\right]}{2 + \frac{\cos 2\theta}{1+4\Omega^2\tau^2} + \frac{\cos 4\theta}{1+16\Omega^2\tau^2}}. \tag{2.8}$$

In the case being considered, $\theta = 109.5°$. Substituting the numerical values of the trigonometric functions involved, we obtain

$$R = -\frac{4\Omega\tau\left[\frac{1,9562}{1+16\Omega^2\tau^2} - \frac{0,6293}{1+4\Omega^2\tau^2}\right]}{2 - \frac{0,7771}{1+4\Omega^2\tau^2} + \frac{0,2079}{1+16\Omega^2\tau^2}}. \tag{2.9}$$

A direct comparison of expression (2.9) with the above experimentally measured value of R leads to the following value of $\Omega\tau$:

$$\Omega\tau = (-4.28 \pm 0.95) \times 10^{-2}. \tag{2.10}$$

This value must be corrected for the finiteness of the solid angles within which gamma radiation is incident to the scatterer and, after a scattering event, to the detector. This correction can be evaluated by comparing the value of R calculated at an angle of $\theta = 109.5°$ with the R value obtained upon averaging over all scattering angles allowed by setup geometry—that is, by the dimensions of the gamma source, detector, and working area of the scatterer, as well as by the corresponding distances. In the case being considered, one may neglect, for the sake of simplicity, the quantities 4 and 16 $\Omega^2\tau^2$ against unity in the denominators of the corresponding terms in expression (2.9). After the introduction of this correction, $\Omega\tau$ proved to be

$$\Omega\tau = (-4.45 \pm 1.00) \times 10^{-2}. \tag{2.11}$$

The half-life of the ^{182}W nucleus in the excited state at 100.1 keV was measured in many studies. A compendium of the results obtained to 1966 inclusive was given in [9], the result averaged over all studies being $T_{1/2} = (1.37 \pm 0.01) \times 10^{-9}$ s. An updated result averaged over studies performed before September 1974 was given in [10]: $T_{1/2} = (1.38 \pm 0.02) \times 10^{-9}$ s. Although it is quite surprising that the accuracy in determining this quantity became worse in the course of time, either value is acceptable for us. Taking the value of $T_{1/2} = (1.38 \pm 0.02) \times 10^{-9}$ s, one obtains $\tau = 1.99 \pm 0.03$ ms, which leads to $\Gamma = (0.530 \pm 0.008) \times 10^{-18}$ erg $= (3.31 \pm 0.05) \times 10^{-7}$ eV. Substituting this value of τ into (2.11), one obtains for Ω the value of $-(2.24 \pm 0.50) \times 10^7$ s^{-1}. From here, one arrives at the g-factor value of 0.346 ± 0.077. The natural width of the excited state in units of the relative velocity of the Mössbauer gamma source and the absorber is (0.0992 ± 0.0015) cm/s.

Direct measurements of the real width of the 100.1 keV gamma line in Mössbauer experiments in transmission geometry were performed in several studies quoted in [5, 6, 11–15]. Those articles either present the directly observed experimental Mössbauer resonance width, which is equal to the sum of the width of the gamma-source (metallic tantalum irradiated with reactor neutrons) emission line, Γ_s, and the width of the resonant-absorber (tungsten metal) absorption line, Γ_a, or other data from which one can extract the value of $\Gamma_s + \Gamma_a$. The average of this sum over the results of the quoted studies is 0.2170 ± 0.0046 cm/s. Under the assumption that the width Δ of the Mössbauer gamma line emitted by metallic tantalum is half this value, one obtains the value of 1.094 ± 0.025 for Δ/Γ.

As a matter of fact, the above value of $\Omega\tau = (-4.45 \pm 1.00) \times 10^{-2}$ is equal to the angle $\Delta\theta$ through which the AD of resonantly scattered gamma rays was rotated in the experiment being discussed. According to the correct theory of magnetic-field-perturbed ADs, this angle is $\frac{(2\Gamma+\Delta)}{(\Gamma+\Delta)}\Omega\tau$ rather than $\Omega\tau$. In our case, we then have $\Delta\theta = 1478\ \Omega\tau$. This means that the value correctly determined from the experiment in question for the g-factor of the ^{182}W nucleus in the 2^+ excited state at 100.1 keV is $(0.346 \pm 0.077)/1.478 = 0.234 \pm 0.052$. These measurements, performed by the present author together with Sorokin, were not published separately. Their results formed the content of Sorokin's thesis completed in 1964 and presented for a diploma. Later, these results were included by the present author in his lecture

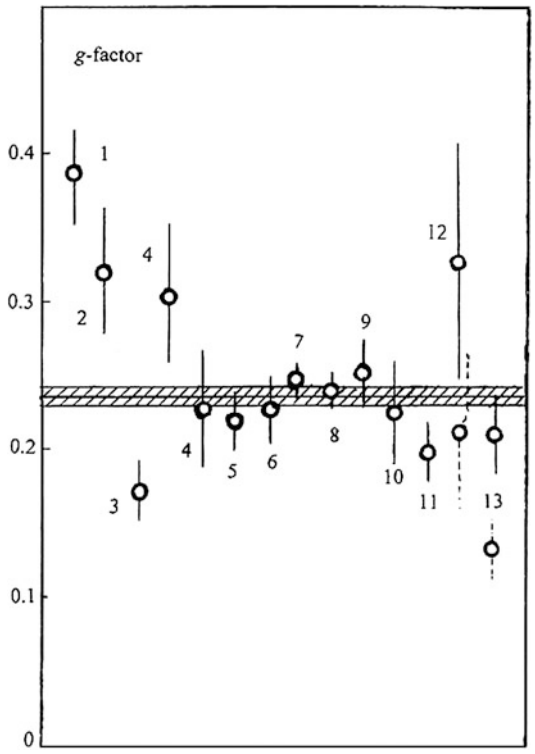

Fig. 2.7 Measured values of the g-factor of the ^{182}W nucleus in the excited state at 100.1 keV from (*1*) [24], (*2*) [25], (*3*) [26], (*4*) [27], (*5*) [28], (*6*) [29], (*7*) [30], (*8*) [31], (*9*) [32], (*10*) [33], (*11*) [15], (*12*) [16], and (*13*) [18]. The g-factor values obtained upon the treatment of data on the basis of the theory that takes into account the ratio of the width of the spectrum of gamma rays that experienced resonant scattering to the natural width of the excited nuclear level are shown by the dotted lines under points 12 and 13. The average g-factor value and the error in it according to calculations based on the g-factor values corresponding to points 4–11 are represented by the horizontal shaded band

delivered at the Winter School in Physics at the Ioffe Leningrad Institute for Physics and Technology in 1970 [16].

Let us now compare the results that we obtained with data of investigations performed by different methods. The g-factor values for the first excited 2^+ state of the ^{182}W nucleus are given in Fig. 2.7 according to studies reported before the completion of our experiment described immediately above. The results of the first three studies deviate strongly from one another and contradict the majority of more recent data. Starting from fourth study (the respective references are given in the caption under Fig. 2.7), however, the g-factor values are quite consistent, and one can use them to calculate of the average g-factor value. It turned out to be 0.258 ± 0.006. The horizontal shaded band in Fig. 2.7 shows this average value and the error in it. They were calculated by using data numbered by integers in the range

from 4 to 11. The g-factor value that we obtained by treating the experimental data according to the theory of angular correlations of sequentially emitted photons –that is, without taking into account the ratio Δ/Γ—is represented by point 12. The value deduced by using the correct theory and the error in this value are shown by the dotted line below point 12. One can see that this value agrees much better with the average g-factor value than the value represented by point 12. Later, I became aware of yet another study, that which was reported in [17] and according to which the g-factor of the state of the ^{182}W nucleus at 100.1 keV is 0.264 ± 0.006. Taking into account this value, together with the data in Fig. 2.7, we arrive at the average g-factor value of 0.261 ± 0.004, which slightly raises the shaded band in Fig. 2.7.

In 1965, there appeared the article of Chow et al. [18], who reported on an experiment where they used a method similar to ours to measure the g-factor for the ^{182}W, ^{186}W, ^{186}Os, and ^{188}Os nuclei. Although those authors treated their data within old strategies—that is, without taking into account the ratio Δ/Γ—they estimated the g-factor for the ^{182}W nucleus at 0.233 ± 0.027 (point 13 in Fig. 2.7), which is close to the average result (in Fig. 2.7) of the studies performed by other methods, which obviously did not require taking into account the ratio Δ/Γ. If one corrects the result from [18] in accordance with requirements of the correct theory, then the corresponding point (0.159 ± 0.018) appears to be considerably lower than the average g-factor value (in Fig. 2.7, this point is shown by the dotted line below point 13). The situation around the other three g-factors measured in [18] is similar, but, for osmium isotopes, especially for ^{188}Os, there is some excess of the measured values over the g-factor values obtained by averaging the results of other studies.

It does not seem possible to explain this situation on the basis of information presented in [18]. There are no reasons to criticize that experiment. However, one of authors of [18] recommended, in his more recent review article [19], to address these data with caution because they were not reproduced. In addition to their main results for the first excited 2^+ states of $^{182,\ 186}$W and $^{186,\ 188}$Os, the authors of [18] also presented the g-factor value for the ^{192}Os nucleus in the 2^+ state at 206 keV according to a measurement in a separate experiment (judging by the energy of this level, without the use of the Mössbauer effect). This result turned out to be at odds with more recent measurements performed by Goldring et al. [20], who indicated that the authors of [18] informed them that their result for ^{192}Os was erroneous. However, it remains unclear whether this also applies to the other results from [18] —in particular, the results for ^{182}W.

2.4 Measurement of the Unperturbed Angular Distribution of Gamma Rays Resonantly Scattered by ^{191}Ir Nuclei

After successful (from our point of view) experiments with ^{182}W, we began studying gamma-ray resonant scattering by ^{191}Ir nuclei that was accompanied by the excitation of the 5/2 level at 129.4 keV. This is the same nucleus and the same transition as those studied by R. Mössbauer himself when he discovered in 1958 the

phenomenon of recoilless gamma-ray emission and absorption [21, 22]. The ADs of resonantly scattered gamma rays of the ^{191}Ir nucleus had not been measured by the time when we began our study. In the course of our work, however, there appeared the article of F. Wittmann [23], who reported on the measurement of ADs for this nuclide. Those measurements were performed for scattering angles not larger than 90°, but our measurements were made for scattering angles from 90° to 150°. As will be seen below, our results turned out to be in good agreement with data from [23], slightly surpassing them in statistical accuracy.

The ADs of 129.4 keV gamma rays experiencing Mössbauer scattering by ^{191}Ir nuclei were measured at the same setup as that which was used in the experiments with ^{182}W [2]. A gamma source was a round pellet 1 cm in diameter from a mixture containing 150 mg of metallic osmium and 350 mg of aluminum powder added in order to increase the mechanical strength of the pellet. The pellet was irradiated for 2 weeks in a flux of reactor thermal neutrons with a density of about 4×10^{13} n/cm^{2}s in an evacuated quartz ampule. The source must be in a tightly sealed cuvette during the irradiation because, in the case of irradiation in open air at elevated temperature, there arises the OsO_4 compound, which is volatile.

The decay scheme for the radioactive isotope ^{191}Os is shown in Fig. 2.8. The intensity of the 82 keV transition is very small in this case, and one uses the parent isotope ^{191}Pt as the source material in order to study the Mössbauer effect with 82 keV gamma rays. The 129.4 keV transition is a mixed $E2 + M1$ transition. The unperturbed angular distribution of gamma rays that experienced resonant scattering accompanied by the excitation of the 129.4 keV level can be represented in the form

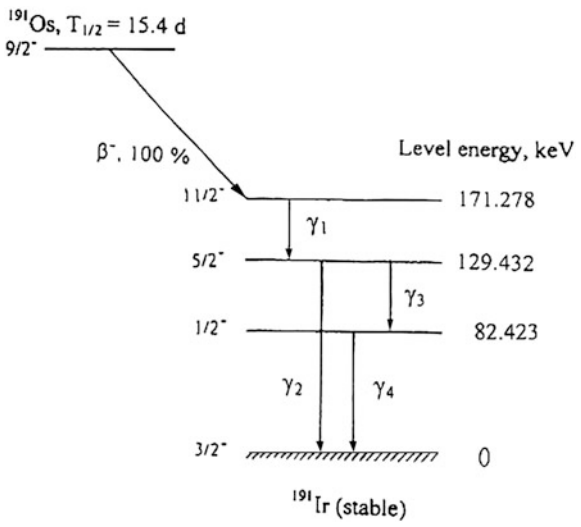

Fig. 2.8 Scheme of ^{191}Os decay and of subsequent transitions in the daughter nucleus ^{191}Ir according to [36]. The total intensities of the γ_1, γ_2, γ_3, and γ_4 transitions (gamma radiation + internal-conversion electrons) per each 100 decay events are 100, 99.4, 0.36, and 0.36, respectively

$$W(\theta) = \sum_{k=0,2,4} B_k B'_k P_k(\cos\theta) = \sum_{k=0,2,4} A_k P_k(\cos\theta), \tag{2.12}$$

where $P_k(\cos\theta)$ are Legendre polynomials, as before, and the coefficients B_k and B'_k are given by

$$B_k = F_k(L_1 L_1 I_i I) + 2\delta_1 F_k(L_1 L_1 + 1\, I_i I) + \delta_1^2 F_k(L_1 + 1\, L_1 + 1\, I_i I), \tag{2.13}$$

$$B'_k = F_k\big(L_2 L_2 I_f I\big) + 2a\delta_2 F_k\big(L_2 L_2 + 1\, I_f I\big) + \delta_2^2 F_k\big(L_2 + 1\, L_2 + 1\, I_f I\big). \tag{2.14}$$

The functions F_k are determined by expression (1.34).

In the case of resonant gamma-ray scattering, we may set $\delta_1 = \delta_2 = \delta$ if, in accordance with the formalism of Dolginov [34], we assume that $a = -1$. In the formalism adopted in [23] (and also in the study that was reported in [35] and which was used as a basis for our computations in Chap. 1), $a = +1$ and the coefficients B_k and B'_k are identical. Historically, the results of our AD measurement for ^{191}Ir were treated on the basis of Dolginov's formalism. As a result, the signs of the multipole-mixture parameter δ for the 129.4 keV transition in our study and in [34] turned out to be different. This circumstance was highlighted in our article quoted in [36] and devoted to describing those experiments.

The numerical values of F_k are such that the products of the coefficients B_k and B'_k in Dolginov's formalism are given by

$$B_0 B'_0 = \big(1 + \delta^2\big)^2, \tag{2.15}$$

$$B_2 B'_2 = \big(0.374 + 1.898\delta - 0.191\delta^2\big)^2, \tag{2.16}$$

$$B_4 B'_4 = 0.497\,\delta^4. \tag{2.17}$$

After dividing both sides of Eq. (2.12) by the constant $B_0 B'_0 = \big(1 + \delta^2\big)^2$, we can recast this equation into the form

$$W(\theta) = 1 + A_2 P_2(\cos\theta) + A_4 P_4(\cos\theta), \tag{2.18}$$

where

$$A_2 = \frac{B_2 B'_2}{B_0 B'_0}, A_4 = \frac{B_4 B'_4}{B_0 B'_0}, \tag{2.19}$$

The procedure for measuring ADs was identical to that in the case of ^{182}W. The number of resonantly scattered photons was determined as the difference of the number of counts in the NaI(Tl) scintillation counter in the cases where the gamma source was at rest and where it oscillated under the influence of the electromagnetic vibrator at a root-mean-square velocity sufficiently high for the disregard of residual

resonant scattering to be legitimate. The geometry of the setup, resonant and nonresonant gamma-ray absorption in the scatterer, and the secondary (Compton) scattering of gamma rays that first experienced Mössbauer scattering were taken into account in the treatment of the data that we obtained. The mathematical aspect of this treatment consisted in selecting, by the maximum-likelihood method, values for the coefficients A_2 and A_4 in expression (2.18) such at which the results of taking into account the aforementioned factors provided the best agreement between the measured and calculated angular distributions. These computations led to the following form of the angular distribution:

$$W(\theta) = 1 + (0.901 \pm 0.041)P_2(\cos\theta) + (-0.042 \pm 0.053)P_4(\cos\theta). \quad (2.20)$$

The graph of this function calculated on the basis of experimental data with allowance for the geometry of the experiment and for the absorption of initial and scattered gamma rays in the scatterer is shown in Fig. 2.9 along with the measured values of this function. In order to extract the value of the multipole-mixture parameter δ from these data, it is necessary to construct graphs representing the dependence of the coefficients A_2 and A_4 on the relative fraction of the $E2$ multipole in the total intensity of the 129.4 keV transition. Obviously, we have

$$\frac{I(\mathrm{E2})}{I(\mathrm{E2}) + I(\mathrm{M1})} = \frac{\delta^2}{\delta^2 + 1}. \quad (2.21)$$

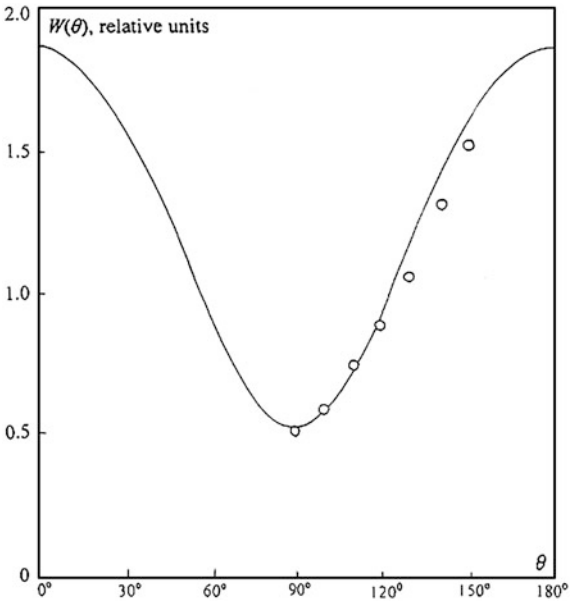

Fig. 2.9 Unperturbed angular distribution of 129.4 keV gamma rays resonantly scattered by ^{191}Ir. The experimental errors are smaller than the size of the *open circles* representing experimental data. The *solid line* was obtained with allowance for the required corrections to the data

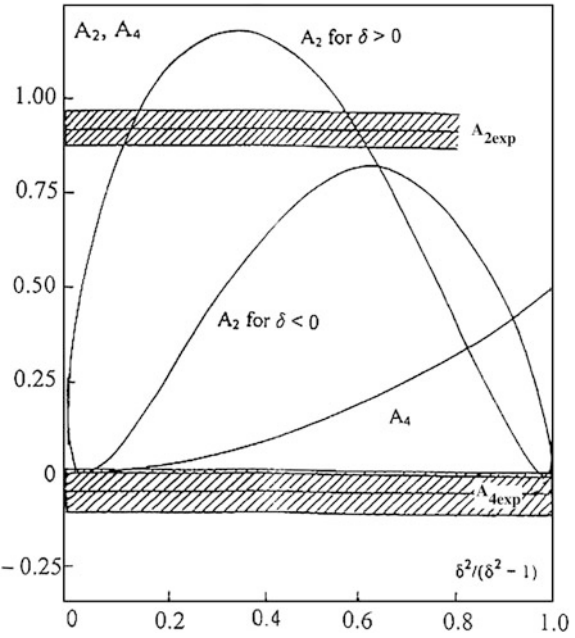

Fig. 2.10 Values found experimentally for the coefficients A_2 and A_4 (these values and the errors in them are shown by the shaded bands), which determine the unperturbed angular distribution of 129.4 keV gamma rays resonantly scattered by ^{191}Ir nuclei, along with the results of theoretical calculations

This ratio changes from 0 to 1 as δ changes from 0 to ∞. In Fig. 2.10, the ratio $\frac{\delta^2}{\delta^2+1}$ is plotted along the abscissa, while the coefficients A_2 and A_4 calculated by formulas (2.19) with allowance for Eqs. (2.15)–(2.17) are plotted along the ordinate.

In this figure, there are two curves for A_2, one for positive and the other for negative values of δ. In the same figure, the values found experimentally for the coefficients A_2 and A_4 are represented by the horizontal dotted lines, while the confidence intervals for these quantities at a 68 % C.L. are shown by the shaded bands. From the intersections of these bands with the theoretical curves, it unambiguously follows that the multipole-mixture parameter for the 129.4 keV transition in the ^{191}Ir nucleus is +0.398 ± 0.020. In [23], a value of $-0.36^{+0.04}_{-0.01}$ was obtained for δ (the reasons for the difference in sign were explained above). Therefore, the two studies in question gave consistent results. It should be noted that the δ value measured in our study was included, as the most precise one, in the tables presented in [37] as an adopted characteristic of the 129.4 keV level of the ^{191}Ir nucleus.

2.5 Measurements of Magnetic-Field-Perturbed Angular Distributions of 129.4 keV Gamma Rays Resonantly Scattered by ^{191}Ir Nuclei in an Ir–Fe Alloy

The main objective of these experiments was to obtain quite convincing data on the role that the hierarchy of the characteristic width of the spectrum of exciting gamma radiation and the natural width of the excited nuclear level plays in experiments devoted to studying the magnetic perturbation of the angular distribution of resonantly scattered gamma rays. A direct check of Eqs. (1.53) and (1.65) must consist in measuring magnetic-field-perturbed ADs for identical nuclei using exciting gamma rays whose spectra have different widths. In principle, this could be achieved by measuring ADs first with the aid of Mössbauer scattering and then with the aid of "classic" resonant gamma-ray scattering—that is, by using first a cooled gamma source and then a heated one. However, it is very difficult to perform this sequence of experiments because nuclei that may be well excited by means of the Mössbauer effect are usually characterized by a very small cross section for "classic" resonant scattering. At the same time, nuclear transitions that are the most suitable for observing "classic" resonant scattering are absolutely useless for Mössbauer experiments because of a high energy of respective photons. It is therefore more convenient to compare the results of measuring, through the observation of the perturbation of ADs with the aid of the Mössbauer effect, the magnetic moment of any nucleus in an excited state with data obtained for this magnetic moment by totally different methods. Nuclei of ^{191}Ir are very convenient for such an experiment for the following reasons:

1. If use is made of metallic iridium as a scatterer material and of metallic osmium as a gamma-source material, then the Mössbauer effect is observed very well even at liquid-nitrogen temperature.
2. The unperturbed AD of 129.4 keV resonantly scattered gamma rays is quite anisotropic (see above).
3. Very high strengths of the internal magnetic field can be obtained in the case of employing Ir–Fe ferromagnetic alloys.
4. Data on the average lifetime of ^{191}Ir nuclei in an excited state at 129.4 keV are available from [38–41]. The natural width of this state can be deduced from these data.
5. There are a number of studies [3, 22, 42, 43] devoted to the Mössbauer effect for ^{191}Ir gamma rays of energy 129.4 keV. Information about the width of the gamma line of exciting radiation can be extracted from their results.
6. Finally, there are some studies that were performed without using the Mössbauer effect and in which consistent data on the magnetic moment of this nucleus in the state at 129.4 keV were obtained.

The layout of the setup used in the experiment being discussed is shown in Fig. 2.11. A gamma source in the form of a pellet 15 mm in diameter consisted of 400 mg of metallic-osmium powder mixed with 600 mg of aluminum powder.

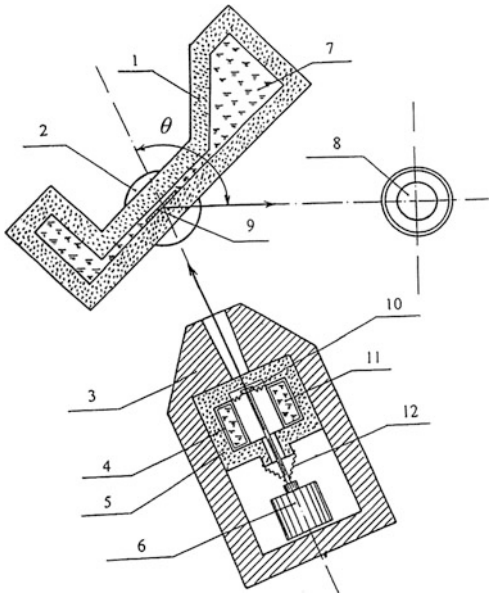

Fig. 2.11 Layout of the setup for measuring perturbed angular distributions of resonantly scattered gamma rays (*top view*): (*1*) Styrofoam container, (*2*) electromagnet pole piece, (*3*) protective "house" formed by blocks from lead and a W-Cu alloy, (*4*) brass container, (*5*) Styrofoam thermal screen, (*6*) electromagnetic vibrator, (*7*) liquid nitrogen, (*8*) Ge(Li) detector, (*9*) scatterer, (*10*) gamma source, (*11*) liquid nitrogen, and (*12*) rubber membrane

This pellet was irradiated for 2 weeks in a thermal-neutron flux of density about 2×10^{13} n/cm^{2}s. After irradiation, the pellet was tightly sealed in a brass ampule with a thin (0.2 mm) front wall. The ampule containing the gamma source was screwed on a spring membrane from beryllium bronze by means of a rod connected to the movable coil of an electromagnetic vibrator. This membrane was mounted on the front face of a horizontal pipe soldered in the lower part of a rectangular brass container for liquid nitrogen. This container was placed in a Styrofoam thermal screen. A detailed structure of the container is shown in Fig. 2.12. In order to cool better the gamma source, which did not have a direct contact with liquid nitrogen, the pipe that removed nitrogen vapor from the container went through the volume of liquid nitrogen from the top of the container to its lower part and came outside near the gamma source. Upon switching on the vibrator, the gamma source could execute nearly sinusoidal oscillations at a frequency of 59 Hz with an amplitude of up to 2.5 mm, which corresponded to the highest velocity value of 78.5 cm/s (in order to shift the Mössbauer gamma line of energy 129.4 keV by its natural width, it was necessary that the source velocity with respect to the absorber be 0.87 cm/s). The entire source–vibrator assembly was covered with a radiation screen formed by blocks from Pb and a W–Cu alloy. The photon beam went out through a lead collimator of rectangular cross section that broadened gradually outward in the horizontal plane. The scatterer of gamma rays was a plate from an Ir–Fe alloy containing 7 wt.% of iridium of natural isotopic composition. The dimensions of the

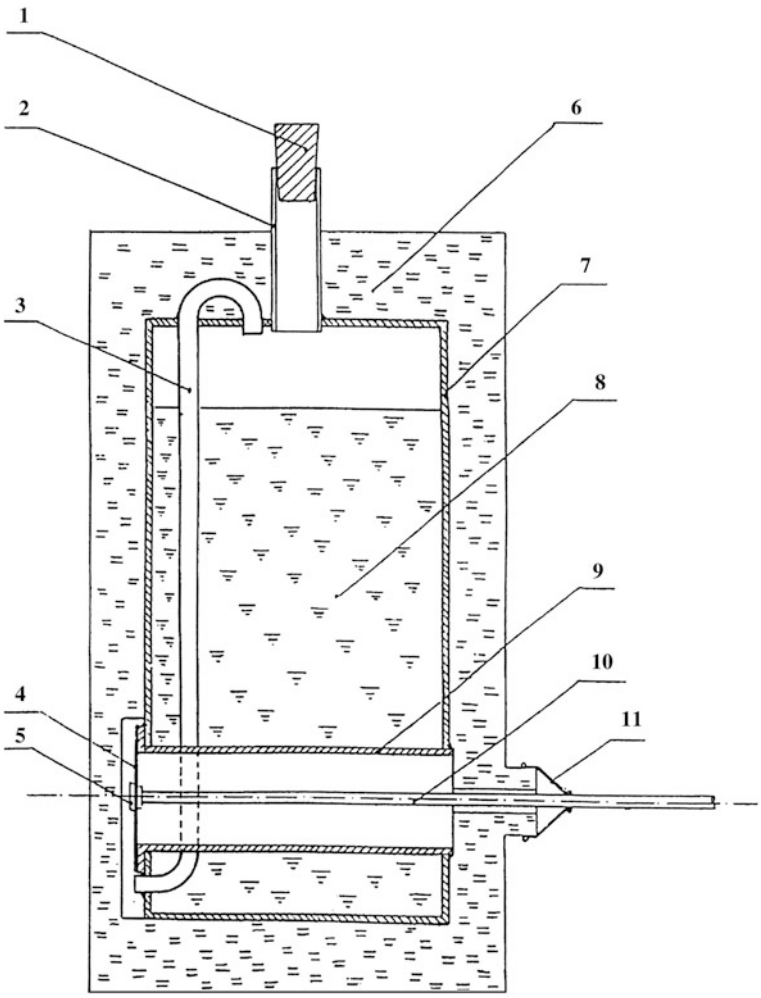

Fig. 2.12 Container for cooling the gamma source used in the experiments devoted to measuring perturbed angular distributions of resonantly scattered gamma rays of ^{191}Ir: (*1*) plug of the pipe for pouring liquid nitrogen, (*2*) pipe for pouring liquid nitrogen, (*3*) pipe for removing nitrogen vapor, (*4*) membrane from beryllium bronze, (*5*) gamma source, (*6*) Styrofoam thermal screen, (*7*) brass body of the container, (*8*) liquid nitrogen, (*9*) brass pipe soldered in the container body, (*10*) rod connecting the gamma source to the movable coil of the electromagnetic vibrator, and (*11*) rubber membrane

plate were 46 × 30 × 1 mm^3. The alloy for the scatterer was fabricated by melting iridium and iron in a nitrogen atmosphere. The sample produced in this way was repeatedly rolled at gradually increasing temperature until the required thickness was achieved. The fabricated plate was polished and cut to the required dimensions, whereupon it was annealed in a vacuum at a temperature of 800 °C for 8 h, the mode of cooling being stepwise. After that, the plate was etched in a mixture of

hydrochloric and nitric acids. An X-ray study revealed the cubic body-centered structure of the alloy. The scatterer was mounted inside a Styrofoam container filled with liquid nitrogen. The back side of the scatterer was directly washed by a liquid-nitrogen layer about 3 mm in thickness. The container central part, where the scatterer was placed, was arranged in between the poles of a small electromagnet that created a field of strength about 1 kOe. A dedicated experiment aimed at measuring the alloy magnetization curve revealed that this was sufficient for magnetizing the scatterer in a specific direction.

Scattered gamma rays were recorded by a Ge(Li) detector belonging to a coaxial type and having an operating volume of about 25 cm^3. The detector was covered with a lead layer from the top and from all sides, with the exception of the side facing the scatterer. A copper filter was used to reduce the detector counting rate associated with X rays generated in the scatterer. The amplitude spectra of pulses from the detector were measured by a Nokia LP 4840 analyzer. The measurement of each spectrum lasted 10 min. For each scattering angle, the spectrum was measured with a vibrator first in the off mode and then in the on mode. In the course of the measurements, the detector remained immobile with respect to the electromagnet and the scatterer, and this ruled out the possibility of variations in the effect of the dissipated magnetic field on its operation. The scattering angle could be changed in the range from 78^o to 143^o by rotating the movable platform on which the gamma source and vibrator were placed together with the collimator and with the radiation screen. The measurements were performed for seven values of the scattering angle, the above range of angles being scanned repeatedly in the direct and reversed directions at a fixed direction of the magnetic field. In all, about 600 spectra were measured for each direction of the magnetic field. Figure 2.13 shows parts of the spectra obtained for the scattering angle of 117.8^o (the sign of the field affecting iridium nuclei is negative). The open circles represent results for the gamma source at rest, while the closed circles (shown in the region of the total-absorption peak for the 129.4 keV gamma line) refer to the oscillating source. A negative sign corresponds to the applied magnetic field that is directed downward with respect to the scattering plane shown in Fig. 2.11. The internal field acting on iridium nuclei is directed upward in this case. The sign indicated here changes in response to the reversal of the applied-field direction and serves for discriminating between the two directions of the scatterer magnetization. This sign should not be confused with a minus sign stably assigned to the internal magnetic field at the positions of iridium nuclei in the Ir–Fe alloy. The meaning of the latter is that the direction of this field is opposite to the direction of the applied magnetizing field.

In the computer- assisted treatment of the measured spectra, the regions near the total-absorption peak for the 129.4 keV gamma line were described by analytic functions depending on several parameters (six to eight for different scattering angles). The very total-absorption peak was assumed to have the instrumental line shape measured in an individual experiment involving a direct irradiation of the detector with gamma rays of ^{191}Ir. The most probable parameter values were determined by using the standard code for minimizing the χ^2 criterion. The position of the total-absorption peak for the 129.4 keV gamma line in terms of the number of

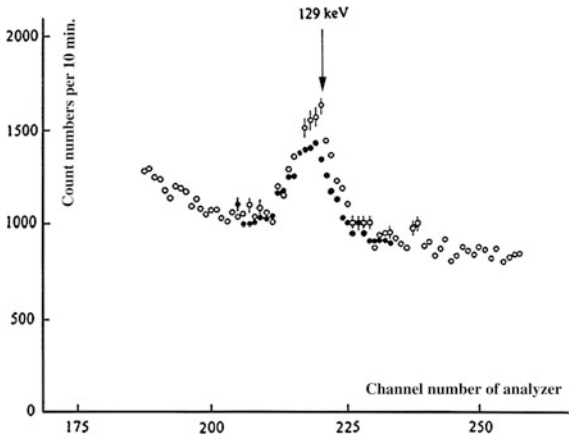

Fig. 2.13 Typical form of those sections of the spectrum of scattered ^{191}Ir gamma rays that contain the total-absorption peak for 129.4 keV gamma rays according to measurements with a 6Ge(Li) detector. The scattering angle was 117.8°. The sign of the magnetic field acting on iridium nuclei is negative. The *open circles* stand for data obtained by using the gamma source at rest, while the *closed circles* (which are shown only in the region of the total-absorption peak for the 129.4 keV gamma line) represent data for the oscillating source. The scale of the errors is indicated by the *vertical bars* at some points

analyzer channels was one of the parameters to be determined. In accordance with the value of this parameter, we evaluated the number of channels, which, in general was a fractional number, but which always corresponded to the same energy interval in which one sums the number of counts associated with the central part of the total adsorption peak (within its FWHM value). Moreover, we calculated the total areas of the total-absorption peaks and the sums of the numbers of counts in control channels lying well above the total-absorption-peak on the energy scale. The control-interval width expressed in terms of channel numbers also depended on the peak position, but it was always on the same energy scale. The ratio of the sums of the numbers of counts in the control channels at a fixed scattering angle for the measurements with the gamma source at rest and with the oscillating gamma source served, after averaging over all measurements, for correcting the numbers of counts at the total absorption peak for the 129.4 keV gamma line with allowance for the possibility that the source-to-scatterer distance may be somewhat different in the two measurement modes (oscillating gamma source versus gamma source at rest). This correction turned out to be very small: the average value of the ratio of the numbers of counts in the control channels for the two measurement modes was 1.00178 ± 0.00043, and we can attribute a significant part of this value to a decrease in the source activity within the time between the starts of two successive measurements in accordance with the usual exponential law of ^{191}Os decay.

The number of resonantly scattered photons was determined for each scattering angle as the difference of the sums of the numbers of counts in the aforementioned

intervals of equally wide (in energy) channels in the area of the 129.4 keV peak in measurements with the vibrator in the off and on modes. The contribution of Rayleigh scattering may be considered to be identical in these two cases because resonant gamma-ray absorption in the scatterer is small in relation to the total absorption and cannot lead to a decrease in the fraction of gamma rays undergoing Rayleigh scattering, as would be the case under conditions of strong resonant absorption [44, 45]. For the same reason, the width of the Mössbauer gamma line shows virtually no increase as radiation penetrates into the interior of the scatterer. Employing the difference of the computer-calculated total peak areas as a measure of the number of resonantly scattered photons proved to be less advantageous if one wants to minimize inaccuracies because an additional subtraction of one large value from another does in fact arise in that case (one first subtracts the computer-calculated pedestal from the sum of the total numbers of counts and then takes the difference of the peak areas obtained upon performing the first procedure). However, the calculated areas of the total-absorption peaks were used to determine independently the ^{191}Os half-life by considering the decrease in these areas over the measurement time (about 10 days for either sign of the magnetic field). This half-life was estimated at 14.60 ± 0.43 d. Together with results of the other studies [46], this value led to an average half-life value of $T_{1/2}(^{191}\text{Os}) = 15.34 \pm 0.32$ d, which was used to introduce corrections for the decay of the source in averaging the results of the measurements.

A further treatment of the experimental results was performed by following method. First, the perturbed angular distributions of resonantly scattered gamma rays were calculated by formula (1.53) for either of the two magnetic-field directions and for twelve presumed values of the g-factor of the ^{191}Ir nucleus in the excited state at 129.4 keV from 0.14 to 0.25. Employing these functions and taking into account setup geometry, gamma-ray absorption in the scatterer, and the dependence of the detection efficiency for gamma rays on geometric conditions of their arrival at the detector, we thereupon calculated the angular distributions of resonantly scattered gamma rays for each g-factor value. Finally, we determined the sought g-factor by comparing the calculated and measured ADs.

In order to calculate perturbed ADs, it is necessary to know, in addition to the g-factor of the nucleus in the excited state being considered, the strength of the internal magnetic field acting on iridium nuclei in the Ir–Fe alloy, as well as the quantities τ, Δ/Γ, and δ and the g-factor of the ^{191}Ir nucleus in the ground state. Figure 2.14 shows data from [47–55] on the dependence of the strength of the internal magnetic field at nuclei of iridium on its concentration in the Ir–Fe alloy at temperatures in the range of $T \leq 4.2$ K. It can be seen that this dependence is satisfactorily described by a linear law. In [48], the magnetic field was measured at room temperature. The H value associated in Fig. 2.14 with that study was rescaled by us to the temperature of T = 4.2 K in accordance with data from [56] on the temperature dependence of the magnetization of pure iron. The least squares method leads to the following result (recall that a minus sign means that the direction of the internal field is opposite to the direction of the magnetizing field):

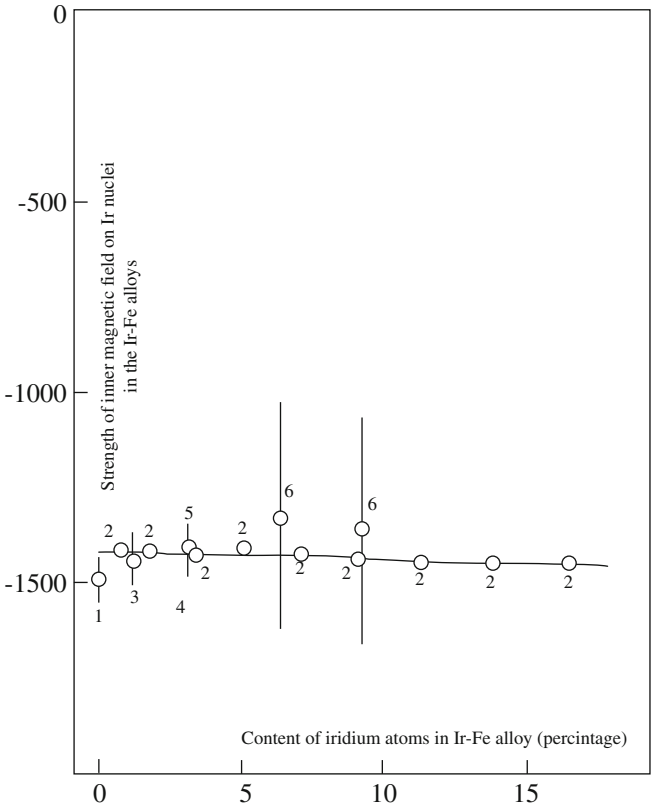

Fig. 2.14 Data on the internal-magnetic-field strength at iridium nuclei in an Ir–Fe alloy as a function of the iridium concentration (in percent): (*1*) averaged result of [47–49, 55]; (*2*) data from [50]; (*3*) averaged result of [51, 52]; and data from (*4*) [47], (*5*) [53], and (*6*) [54]. The errors in the data from [50] are so small that they cannot be shown in this figure. The *solid line* represents the least squares fit of a linear function to the data in the figure

$$H = -(1409.1 \pm 4.3) - (0.73 \pm 0.46) \times C_{Ir}\text{kOe}. \tag{2.22}$$

Here, the iridium concentration is expressed in atomic-percent units. In our case, formula (2.22) gives $H = -1414.2 \pm 5.4$ kOe. In this value, it is necessary to introduce a correction associated with the fact that the experiment was performed at liquid-nitrogen temperature, while expression (2.22) corresponds to temperatures in the range of $T \leq 4.2$ K. In order to introduce this correction, we employed data on the temperature dependence of the internal magnetic field at iron nuclei in pure iron [56],

assuming that this dependence survives for the internal field at nuclei of a small admixture of iridium in iron. This assumption is based on published data on the temperature dependence of internal magnetic fields for a whole series of admixed atoms in ferromagnetic substances [57] and also on the influence of admixtures on the temperature dependence of the field at nuclei of ferromagnetic substances [58]. From these data, it can be seen that a deviation of the temperature dependence of the field at admixed nuclei from the respective dependence of the field at nuclei of a pure ferromagnetic material, if any, is observed only at temperatures higher than (0.2–0.3) T_{Curie} for this ferromagnetic material and is not greater in these cases than several percent.

Therefore, an anomalous temperature dependence of the internal magnetic field at iridium nuclei in iron should not be expected in our case (T = 77 K). Existing experimental data on iridium nuclei admixed to nickel [44] support this point of view.

After introducing the temperature correction, we obtain $H = -1411.0 \pm 5.4$ кOe. It is necessary to subtract the external- magnetizing-field strength of 1 kOe from this value since the external field is opposite in direction to the internal field. Ultimately, we have $H = -1410.0 \pm 5.4$ kOe.

The averaging of data from studies performed without employing the Mössbauer effect [38–41] leads to the following value of the mean lifetime of the ^{191}Ir nucleus in the excited state at 129.4 keV: $\tau = (1.753 \pm 0.085) \times 10^{-10}$ s. This value and the results obtained by measuring the width of the 129.4 keV Mössbauer gamma line [3, 22, 42, 43] give $\Delta/\Gamma = 1.351 \pm 0.050$. The parameter characterizing the mixture of $E2$ and $M1$ multipoles for the 129.4 keV transition was evaluated by averaging the results quoted in [37] and obtained in several studies, including our study reported in [36]. The resulting multipole-mixture parameter is $\delta = -0.4020 \pm 0.0038$. In accordance with [59], the g-factor value for the ground state of the ^{191}Ir nucleus was taken to be $g_0 = 0.09687 \pm 0.00040$. On the basis of data from [60], one can neglect the isomeric shift between the emission line of a source from metallic osmium and the absorption line of a scatterer, which is a plate from an Ir–Fe alloy.

With the aid of precisely these constants, the aforementioned perturbed angular distributions were calculated for 12 values of the g-factor for the ^{191}Ir nucleus in the state under investigation and for two directions of the magnetic field acting on iridium nuclei. Each such function was computed at 116 scattering angles, this being done with a step of one degree in the interval from 60° to 167°. After that, these functions were used to calculate the ADs of scattered gamma rays, and the results could be compared directly with measured ADs. This was done with allowance for setup geometry—that is, the dimensions of the source, scatterer, and detector and the distances between them and for gamma-ray absorption as they penetrate into the interior of the scatterer and escape from it. Moreover, we took into account the dependence of the efficiency of the coaxial germanium detector on the geometric conditions of the arrival of photons at it. This was dictated by the need for taking into account the absorption of gamma rays in the outer “dead” layer of the detector and their passage through the inoperative region of the inner core in the body of the detector. All this required computing, for each of seven scattering angles for which we measured the intensity of scattered gamma rays, sevenfold

integrals with respect to two coordinates in the gamma-source plane, three coordinates of scatterer-volume elements, and two coordinates of the points at which photons hit the detector. The g-factor value for the ^{191}Ir nucleus in the excited state under study was determined individually for either magnetic-field direction by minimizing the χ^2 criterion in comparing measured ADs with a set of 12 computed ADs. We varied two parameters: the g-factor value and the ordinate scale, which was used to level the measured and calculated ADs. For the two signs of the magnetic field, we obtained the following values of the g-factor:

for the case where the external field is positive.

$$g = 0.206 \pm 0.035$$

for the case where the external field is negative and

$$g = 0.195 \pm 0.017$$

The average result is

$$g = 0.197 \pm 0.015$$

The errors indicated here are associated exclusively with the statistics of the number of counts. Upon taking into account the errors in τ, H, δ, Δ/Γ, and g_0, the final result becomes

$$g = 0.197 \pm 0.018. \tag{2.23}$$

The results of the measurements and calculations are shown in Fig. 2.15. The theoretical angular distributions calculated by formula (1.53) for the g-factor values obtained in the way outlined above are represented by the solid curves. These curves are slightly asymmetric with respect to an angle of $\theta = 90°$, because the measured g-factor values are different in these two cases. The dashed lines stand for the angular distributions calculated with allowance for setup geometry, gamma-ray absorption in the scatterer, and the geometric dependence of the detector efficiency. The degree of their agreement with experimental data is determined by the following values of the χ^2 criterion:

$$\text{for curve } 1^{a}, \quad \chi^2 = 7.90;$$
$$\text{for curve } 2^{a}, \quad \chi^2 = 5.95.$$

The number of the degrees of freedom is five in each case—that is, the expected value of the criterion must satisfy the condition $\chi^2 = 5.0 \pm 3.2$. Therefore, the description of experimental data by the curves calculated with the above values of the parameter g is quite satisfactory.

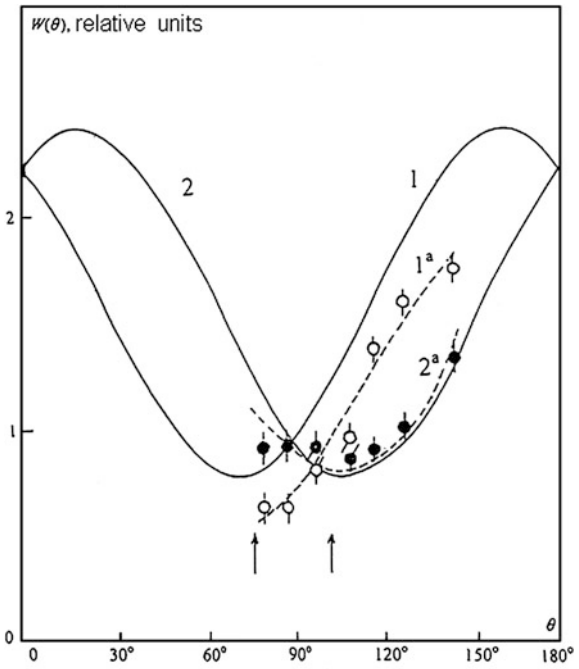

Fig. 2.15 Results of measurements and calculations for magnetic-field-perturbed angular distributions of 129.4 keV gamma rays resonantly scattered by ^{191}Ir nuclei in an Ir–Fe alloy. *Curves* 1 and 1^a and the *open circles* refer to a positive sign of the external magnetic field, while 6 the remaining data correspond to its negative sign. The *dashed curves* 1^a and 2^a represent the most probable angular distributions calculated on the basis of experimental data with allowance for the geometry of the experiment, gamma-ray absorption in the scatterer and the detector efficiency. The *solid curves* 1 and 2 were calculated by formula (1.53) with the optimum g-factor values that we obtained for the two signs of the magnetizing field. The normalizations are different for the pair of *curves* 1 and 2 and the pair of *curves* 1^a and 2^a. The *arrows* indicate the expected positions of the minima of the angular distributions for the case where their rotation angles are calculated by the formula $\Delta\theta = \Omega\tau$

The results of three studies that were performed before the completion of our experiment without employing the Mössbauer effect and in which the g-factor was measured for the ^{191}Ir nucleus in the excited state of our interest are given in Table 2.1. In order to average these data and to compare the averaged result with the g-factor value that we measured, it is necessary to rescale these three g-factor values to the same average lifetime that we adopted for the ^{191}Ir nucleus in the excited state. This is necessary because experimental data give the quantity $\Omega\tau = -g\mu_N H\tau/\hbar$ rather than the g-factor proper, so that the resulting g-factor value depends on the value adopted for τ. The averaging of rescaled g-factor values yields

Table 2.1 The g-factor values of the 129.4 keV state of ^{191}Ir nuclide measured without of Mössbauer effect

References	Method of measurement	τ value adopted by the authors for the level at 129.4 keV	g-factor value obtained for the ^{191}Ir nucleus in the state at 129.4 keV
Avida et al. [67]	Perturbed angular distribution of gamma rays after Coulomb excitation	$(1.89 \pm 0.14) \times 10^{-10}$ s	0.23 ± 0.04
Owens et al. [55]	Perturbed angular correlation of sequentially emitted gamma rays	$(1.44 \pm 0.10) \times 10^{-10}$ s	0.22 ± 0.02
Il'khamdzhanov et al. [68]	The same	1.82×10^{-10} s	0.24 ± 0.03

$$g = 0.203 \pm 0.015. \tag{2.24}$$

One can see that this value agrees well with our result, there more so as, there is no need in this comparison, for taking into account the error in τ since it enters into both values under comparison. Good agreement between the values in (2.23) and (2.24) indicates that our method for studying the magnetic hyperfine interaction of excited nuclei on the basis of the magnetic-field-induced perturbation of the AD of gamma rays resonantly scattered via the Mössbauer effect gives correct results if, in treating experimental data, one takes into account the ratio Δ/Γ, as is required by the theory expounded in Chap. 1.

The results of this experiment are a direct experimental indication that, under the excitation conditions prevalent in the case being considered, the mean duration of the precession of excited ^{191}Ir nuclei in a magnetic field, or, what is evidently the same, the mean time within which this nucleus remains in the excited state, exceeds substantially the mean lifetime of excited nuclei, τ, that is determined by the relation $\tau = \hbar/\Gamma$. In order to prove this, we can compare the observed (in our experiment) shift of the minimum of the perturbed AD in relation to the position of the analogous minimum in the unperturbed AD (see Fig. 2.15) with its counterpart following from the usual theory of angular correlations, which does not take into account the role of the width of the spectrum of exciting gamma rays. The averaging of the g-factor value for the 129.4 keV state in (2.24) with the value obtained in our experiment leads to the following result:

$$g_{av.} = 0.201 \pm 0.012. \tag{2.25}$$

From here, it follows that, under conditions of our experiment, the Larmor frequency of the precession of excited nuclei was

$$\Omega = -g\mu_N H/\hbar = (1.324 \pm 0.074) \times 10^9 \text{ s}^{-1} \tag{2.26}$$

The errors in the quantities g and H were taken into account here.

According to the theory of angular correlations that does not take into account the role of the ratio Δ/Γ, the angular shift of the minimum of the curve representing the perturbed AD with respect to its position in the case where there is no magnetic field must be equal to $\Omega\tau$. In the case being considered, this yields

$$\begin{aligned}\Delta\theta = \Omega\tau &= (1.324 \pm 0.074) \times 10^9 \times (1.753 \pm 0.085) \times 10^{-10} \\ &= 0.232 \pm 0.017 \text{ rad} = 13.29 \pm 0.96^\circ,\end{aligned} \tag{2.27}$$

but the actual shifts of the AD minima (they were determined from the solid curves in Fig. 2.15) exceed the above value of $\Delta\theta$ by a factor of 1.40 ± 0.11. The actual lifetime of the nuclei in the excited state exceeds by the same factor the quantity τ under conditions of the experiment being discussed. The above theory of perturbed ADs predicts, on the basis of the known ratio Δ/Γ (which is 1.351 ± 0.05 in the case being considered), a value of 1.425 ± 0.009 for the average lifetime of excited nuclei.

Thus, our experiments confirm fully the conclusion of the theory of perturbed ADs that the average lifetime of nuclei in an excited state depends on the form of the spectrum of exciting gamma rays. The results of this study were presented in our articles quoted in [61, 62].

It was indicated in [63] (p. 160) that, after the publication of our study in [61], the theoretical prediction that the result of perturbing, by a magnetic field, the AD of resonantly scattered gamma rays depends on the width of the spectrum of gamma rays undergoing scattering were also confirmed in [64] (to be published), but I could not find that publication. It was not mentioned in the last review of data on ^{191}Ir nuclide [65] either.

Experimental data obtained in [66] by using gamma rays of the ^{57}Fe nuclide also furnish an explicit piece of evidence confirming the above conclusion that the lifetime of a nucleus in an excited state depends on excitation conditions—in particular, on the shift of the exciting Mössbauer gamma line with respect to the position of the excited-nucleus resonance. Among other things, the dependence of the number of counts in the resonance detector on the time t that passed from the opening of a fast shatter for the Mössbauer gamma line of energy 14.4 keV was measured in that study. This dependence must be described by a function of the form $1—e^{-t/\tau}$, where τ is the average lifetime of a nucleus in an excited state.

The measurements were performed at the shifts s of the exciting gamma line with respect to the absorption line that were equal to 0, Γ and 2.5 Γ (Γ is the natural width of the state to be excited). The results of these measurements are presented in Fig. 2.16. The second and third columns of Table 2.2 give, respectively, the τ values obtained by the authors of [66] from experimental data and the τ values calculated by formula (1.86). One can see that the τ values obtained experimentally are very close to those expected theoretically.

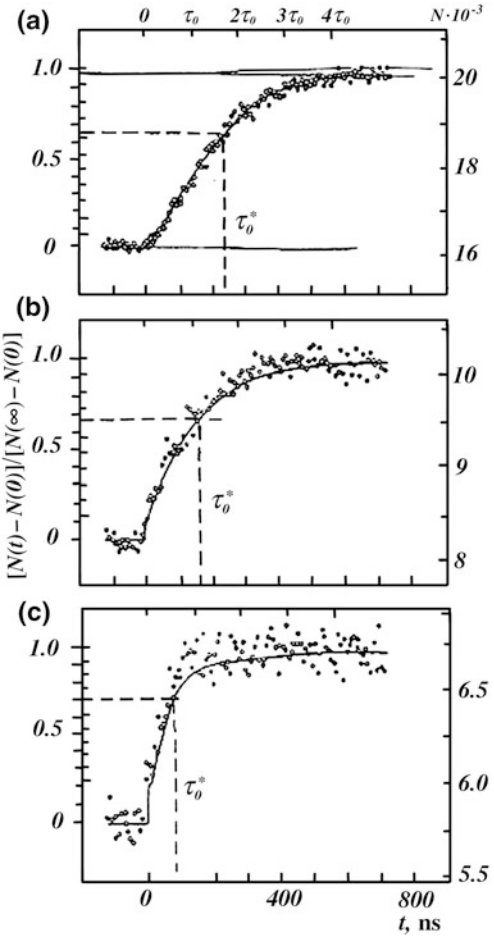

Fig. 2.16 Experimental data from [66] that confirm the above theoretical conclusions (Eq. 1.86) on the dependence of the average time within which the nucleus remains in the excited state, τ_0^*, on the energy shift of the exciting Mössbauer line with respect to the position of the resonance of absorber nuclei. The numbers of counts in the resonance detector for 14.4 keV ^{57}Fe gamma rays are plotted along the ordinate versus the time that passed from the instant at which the fast shatter was opened for these photons. The detector records photoelectrons created in the interactions of all gamma rays emitted by the source with detector atoms and conversion electrons emitted by ^{57}Fe atoms in the detector after the resonant absorption of 14.4 keV photons. The right scale corresponds to the total counting rate in the detector, while the left scale corresponds to the counting rate for conversion electrons alone. The coordinates of the points corresponding to the time τ_0^* that elapsed from the instant at which the shatter was opened are indicated by the *dashed lines* and the symbol τ_0^*

Table 2.2 The values of mean lifetime of the 14.4 keV state of ^{57}Fe nuclide independence on the shift s of exciting gamma line measured in [66] and calculated by formula (1.86)

s	$\tau_{exp.(ns)}$	$\tau_{calc.\ (ns)}$
0	230 ± 10	211.5
Γ	160 ± 15	141
2.5Γ	78 ± 15	90

The difference of the experimental and calculated values, which exceeds slightly the errors fotheshift s equal to 0 and Γ, is most likely due to some unrevealed systematic uncertainties. It is noteworthy, however, that the authors of [66] interpret their results from a different point of view, assuming that the theory relating the average lifetime of a nucleus in an excited state to the form of the spectrum of exciting gamma rays is correct in the case of a "stationary" measurement regime in which our experiments with ^{182}W and ^{191}Ir were apparently performed, but it is inapplicable in the case of "nonstationary" regime. However, our "stationary" regime is such that the mean time interval between the instants at which photons hit the detector exceeds considerably the duration of the process of resonant photon absorption in the scatterer; therefore, it does not differ in dynamics from the processes that occur after the opening of the shatter in the experiments described in [66]. We note that the decay of absorber nuclei that was observed by the authors of [66] and which was characterized by the $(e^{-t/\tau})$ law natural for the nuclei in question irrespective of the shift of the source gamma line is possible only under the condition that the distribution of excitation energies of absorber nuclei has, in all cases, a Lorentzian shape with a width Γ, but this may be so only if the spectrum of exciting gamma rays has a width exceeding Γ considerably. Under conditions of the experiment being discussed, this may mean that the main part of absorber nuclei that proved to be in an excited state after the interruption of the gamma beam was excited by photons whose wave trains were cut off (shortened) by shatter-operation events.

Let us now consider the question of possible deviations from the parallelism of the strength vector of the internal magnetic field at nuclei of some admixed atoms in a ferromagnetic material and the strength vector of the external magnetic field magnetizing this ferromagnet [69]. The assumption that there may exist such deviations from the parallelism (antiparallelism in the case of a negative internal field) in question stemmed from the fact that, in a number of experiments, the hyperfine-interaction energies measured by using internal magnetic fields turned out to be systematically lower than the values that followed from experiments performed with the same nuclei by using external magnetic fields and nonmagnetic substances. Such data fitted satisfactorily in the scheme according to which the strength vectors of the internal magnetic field at nuclei of admixed atoms in a polycrystalline ferromagnet lie along the generatrices of a cone whose axis is aligned with the strength vector of the external magnetic field. In some cases, half of the cone opening angle (or the angle between the directions of the internal and external fields) may be 25°–30° at a magnetizing-external-field strength of about 1 kOe. Although such a magnetic-field strength was sufficient for magnetizing the

ferromagnet almost completely, it was not sufficient for orienting the internal field at nuclei of admixed atoms along the direction of the external field. A nearly complete alignment of the field directions (or their nearly perfect antiparallelism in the case of a negative internal field) was reached at an external-field strength as high as about 15 kOe. A qualitative model that is intended for describing the emergence of this phenomenon, but which is not claimed to be highly precise, was proposed in [70]. According to this model, the introduction of an alien atom in the crystal lattice of a ferromagnet generates (mainly because of the difference in the size between this atom and host-material atoms) additional intracrystalline interactions (in particular, magnetostriction interaction), with the result that the magnetization of the substance in the immediate vicinity of the admixed atom differs from the average magnetization of the whole block of the substance. A deviation from the parallelism of the internal magnetic field at the nucleus of the admixed atom and the external field is a manifestation of an unsaturated magnetization of the substance in the vicinity of the admixed atom. All experiments in which indications of this phenomenon were obtained were performed under such conditions that the nuclei under study occurred in a ferromagnet as a result of preceding nuclear processes (for example, the penetration of recoil nuclei after Coulomb excitation or the formation of excited nuclei after beta decay). Under conditions of our experiment, there were no transient processes associated with the appearance of the nucleus under study in the ferromagnet immediately before the event of detection of the experimentally observed effect (in our case, resonant photon scattering). Iridium atoms were introduced in iron at the stage of manufacturing the alloy and were at their preassigned places in the course of the experiment (at crystal-lattice sites, as was shown via an X-ray analysis of the scatterer). They did not experience recoil or exchange phonons with the crystal lattice because resonant absorption proceeded via the Mössbauer effect. Unfortunately, no experiments that could show the presence or absence of an unsaturated magnetization of the substance in the vicinity of admixed atoms under such conditions have been performed thus far. If this effect exists (it can exist in our case because iridium atoms differ in size from iron atoms), then allowance for it must lead to some increase in the g-factor value measured by us for the ^{191}Ir nucleus in the state at 129.4 keV. At the same time, the conclusion that the time within which the nucleus remains in the excited state increases in relation to τ remains valid because this conclusion follows from the observed positions of the minima in the AD of resonantly scattered gamma rays: these positions differ from those that would correspond to the case where the average lifetime of the nucleus in the excited state is τ.

In order to estimate roughly the change in the g-factor value upon taking into account the deviation from the parallelism of the internal and external fields, we consider qualitatively the influence of magnetic fields not parallel to the normal to the scattering plane on the AD of resonantly scattered gamma rays. In Fig. 2.17, q_1 and q_2 are the wave vectors of, respectively, exciting and scattered photons and z is the direction of the normal to the scattering plane. The strength vector $\boldsymbol{H}$ of the internal magnetic field acting on the scattering nucleus is decomposed into two components: $\boldsymbol{H}_{vert.}$ and $\boldsymbol{H}_{horiz}$. The first of them causes the usual perturbation of ADs,

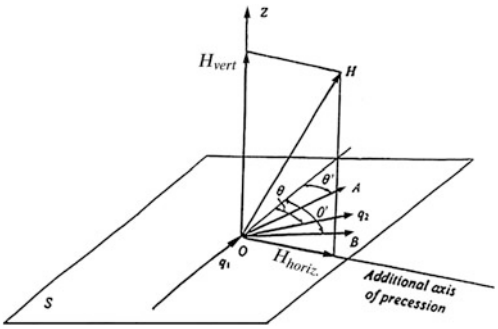

Fig. 2.17 Scheme clarifying the effect that a magnetic field not perpendicular to the scattering plane exerts on the angular distribution of resonantly scattered gamma rays. The explanations to the figure are given in the main body of the text

which is described by formula (1.53), while the second causes an additional precession of the nuclear spin about its direction. Owing to this precession, photons that, in the absence of a magnetic field, would be emitted by nuclei situated near the point *O,* for example, along the straight line *OA* lying outside the scattering plane *S* shown in Fig. 2.17 (or along the straight line *OB* in the case of the different precession direction) will find their way to the detector. The intensities of such gamma rays are determined by the scattering angle θ', which exceeds slightly the angle θ. In response to the reversal of the sign of the magnetizing field, the vector $\boldsymbol{H}$ also changes direction. The precession of nuclear spins about the axis aligned with $\boldsymbol{H}_{horiz}$ also has an opposite direction, with the result that gamma rays that, in the absence of a field, would be emitted along the straight line *OB* find their way to the detector. Their intensity is determined by the same angle θ' because the angle of AD rotation does not depend on the sign of Ω. Thus, the horizontal component of the internal magnetic field acts identically in the two cases: it changes the intensity of resonantly scattered gamma rays as if the scattering angle increases slightly in relation to its adopted geometric value. As a result, the Ω value measured for one sign of the external field is slightly overstated; for its opposite sign, it is understated by nearly the same value. The averaging of the results obtained by measuring ADs for two signs of the external field must lead to a nearly complete elimination of the effect of the horizontal magnetic-field component. If the vectors $\boldsymbol{H}$ lie at the generatrices of the cone whose axis coincides with *z,* then the horizontal projections of these vectors fill uniformly the circle whose center is at the point *O*. It is quite obvious that this set of horizontal projections will remain unchanged after the reversal of the external-field direction. The effect of this set of projections, whatever it may be, must vanish upon averaging the results of the measurements for two signs of the external field. Therefore, a decrease in the effective strength of the magnetic field perturbing ADs and appearing in expression (1.53) is the only important consequence of the deviation from the parallelism of the internal and external fields—namely, $H_{eff} = H_{vert} = H\cos\beta$.

Since the g-factor and $H_{eff.}$ appear in Ω as factors, which cannot be determined individually under conditions of the experiment being discussed, a decrease in one of them implies the respective increase in the other if Ω remains invariable.

If one accepts that, under conditions of our experiment, the angle β is about 25° at H_{ext} = 1 kOe [71], then the g-factor value appears to be 0.217 ± 0.020 instead of 0.197 ± 0.018 (2.13). The result that one obtains by taking the average over the studies reported in [55, 67, 68] and with which we compared our g-factor value will also change because the authors of [55, 68] also employed an Ir–Fe alloy, so that it is also necessary to introduce a correction in their data that would take into account the deviation from the parallelism of the internal and external fields. After the introduction of this correction, the average result of [55, 67, 68] becomes $g = 0.230 \pm 0.010$. Thus, good agreement between the two values under comparison survives after taking into account the deviation from the parallelism of the internal and external fields at iridium nuclei.

Over the time that elapsed from the completion of the aforementioned experiments with the Ir nuclide, there appeared several publications [72–75] that reported on new results of measurements of both the average lifetime of this nucleus in the excited state at 129.4 keV and the g-factor of this state. However, these results look quite contradictory. The tables of nuclear magnetic moments in [72] present a value of $T_{1/2} = (1.29 \pm 0.04) \times 10^{-10}$ s as the recommended half-life of the state of the ^{191}Ir nucleus at 129.4 keV [from here, $\tau = (1.86 \pm 0.06) \times 10^{-10}$ s] and two values for the magnetic moment of this state: 0.450 ± 0.023 and 0.485 ± 0.044 nuclear magnetons (the latter is our result obtained in [62] and rescaled with allowance for the $T_{1/2}$ value adopted in those tables). The average magnetic moment following from these data is 0.458 ± 0.020 nuclear magnetons, which corresponds to a g-factor value of 0.183 ± 0.008.

In [73], the average lifetime of the ^{191}Ir nucleus in the excited state of interest was determined by measuring the dependence of the ratio of the intensity of the gamma line shifted via the Doppler effect to the intensity of the unshifted line on the mean free path of recoil nuclei after Coulomb excitation. It turned out to be $(1.776 \pm 0.060) \times 10^{-10}$ s, which is very close to the value that we used. The g-factor of the 129.4 keV state was measured in that study by two methods: by using the perturbation of the angular distribution of gamma rays by the transient magnetic field acting on ^{191}Ir nuclei that, after undergoing Coulomb excitation, traverse the magnetized iron and by using the perturbation of the angular distribution of gamma rays by the transient magnetic field acting on ^{191}Ir nuclei that, after undergoing Coulomb excitation, traverse the magnetized iron and by using the perturbation of the angular distribution of gamma rays by the static magnetic field acting on nuclei stopped in magnetized iron. The resulting value was $g = 0.180 \pm 0.009$ in the first case and $g = 0.172 \pm 0.013$ in the second case. It is likely that corrections for the deviation from the parallelism of the internal and the magnetizing field must be introduced in these values. One can see that these g-factor values are close to the value obtained in our experiment. However, a different research group, who used a similar method, reported [74, 75] data that were in a glaring contradiction with the results of almost all of the studies performed by the usual methods involving the application of static

magnetic fields. Specifically, g-factor values of 0.342 ± 0.024 and 0.322 ± 0.022 are presented in [74, 75], respectively, for the 129.4 keV state of the ^{191}Ir nucleus. The value obtained in [75] for the average lifetime of the ^{191}Ir nucleus in this excited state is $(1.268 \pm 0.023) \times 10^{-10}$ s, which contradicts the results of the majority of previous studies, including the result presented in [73]. It turns out that the situation is unfavorable not only in the Danish kingdom. I am inclined to the opinion that data obtained under stationary conditions are more reliable since the values of effective magnetic fields are quite certain in that case and since average lifetimes of excited nuclei are then measured by the reliable method of γ–γ and β–γ coincidences. Our data agree well with data obtained by these methods.

2.6 Some Special Features of Gamma-Radiation Processes as Suggested by the Foregoing Analysis

Stepanov and Zipenyuk indicate in [76], referring to the book by Migdal [77], that the duration of the process of photon emission from a nucleus [and, hence, of the process of resonant photon absorption by a nucleus (author)] is about $\lambda\!\!\!^{-}_{\gamma}/c$, where $\lambda\!\!\!^{-}_{\gamma}$ is the gamma-radiation wavelength divided by 2π and c is the speed of light. For gamma rays of energy about 100 keV, this quantity is about 3×10^{-20} s. We will now show that there are reasons to doubt that the duration of such processes is so short. For this, we calculate the average lifetime of nuclei in the excited state populated after Mössbauer resonant photon absorption, assuming that the time of absorption is much shorter than $\tau = \hbar/\Gamma$. For this purpose, one can make use of the quantum-mechanical Krylov–Fock theorem [78], which states that the decay law for an excited quantum system is determined completely by the excitation-energy distribution in the initial state. In the case of an"ideal" Mössbauer resonant gamma-ray scattering, the emission and absorption gamma lines are characterized natural widths, are not shifted with respect to each other, and are described by the Lorentzian function

$$F(E_\gamma) \approx \frac{\Gamma^2/4}{(E_\gamma - E_0)^2 + \Gamma^2/4}, \tag{2.28}$$

where E_γ is the photon energy and E_0 is the position of the resonance center. The excitation-energy distribution $W(E_\gamma)$ of nuclei excited upon the resonant absorption of such photons is proportional to the product of two functions in (2.28); that is,

$$W(E_\gamma) \approx \frac{\left(\Gamma^2/4\right)^2}{\left[(E_\gamma - E_0)^2 + \Gamma^2/4\right]^2}. \tag{2.29}$$

This function is no longer a Lorentzian function; therefore, one cannot expect that the decay of an excited nuclear state will follow the exponential law. The spectrum of photons emitted by excited nuclei will have the same form. One can prove that the FWHM of the gamma line described by expression (2.29) is smaller than Γ by a factor of about 1.5. From this fact alone, it follows that the average lifetime of nuclei in an excited state, t_{av}, must be longer than τ by a factor of about 1.5. But from the rigorous theory described above, it follows, as we have already seen, that the relation $t_{\mathrm{av}} = 1.5\ \tau$ holds exactly. According to the Krylov–Fock theorem, the probability $L(t)$ for an excited system to remain undecayed after the lapse of the time t from its creation is determined by the excitation-energy distribution $W(E_\gamma)$ formed upon the emergence of the excitation within a time short in relation to τ and is given by

$$L(t) = \left| \int e^{-i\frac{E_\gamma}{\hbar}t} W\left(E_\gamma\right) dE \right|^2. \tag{2.30}$$

If we take expression (2.20) for $W(E_\gamma)$, it is necessary to calculate the modulus squared of the integral

$$I = \left(\frac{\Gamma^2}{4}\right)^2 \int_{-\infty}^{\infty} \frac{e^{-i\frac{E_\gamma}{\hbar}t}\, dE_\gamma}{\left[\left(E_\gamma - E_0\right)^2 + \Gamma^2/4\right]^2}. \tag{2.31}$$

The integral is evaluated by taking the residue at the second-order pole in the lower half-plane. Omitting factors independent of t, one obtains

$$L(t) \approx \left(2 + \frac{\Gamma t}{\hbar}\right)^2 e^{-\frac{\Gamma t}{\hbar}}. \tag{2.32}$$

The number of decays per unit time at the instant t is determined by the time derivative of the function $L(t)$:

$$\frac{dL(t)}{dt} = -\frac{\Gamma^2 t}{\hbar^2}\left(2 + \frac{\Gamma t}{\hbar}\right) e^{-\frac{\Gamma t}{\hbar}}. \tag{2.33}$$

The average lifetime of nuclei in an excited state turns out to be

$$t_{\mathrm{av}} = \frac{\int_{-\infty}^{\infty} t\frac{dL(t)}{dt}dt}{\int_{-\infty}^{\infty} \frac{dL(t)}{dt}dt} = 2.5\frac{\hbar}{\Gamma} = 2.5\tau \tag{2.34}$$

instead of 1.5 τ, a result that follows from the width of the gamma line emitted by the scatterer; from the theory of magnetic-field-perturbed angular distributions of resonantly scattered gamma rays; and, finally, from the experimentally measured angle of rotation of the rosette of such an angular distribution of resonantly scattered ^{191}Ir gamma rays. This was first indicated in our article quoted in [79]. It is noteworthy that the experimental value obtained in our study for t_{av} differs by ten standard deviations from the t_{av} value given by the Krylov–Fock theorem. This result is likely to be sufficient for disproving the statement that, in the process of "ideal" Mössbauer resonant scattering, the nucleus involved absorbs (and, hence, emits) a photon within a time that is short in relation to τ. As a matter of fact, the result in question indicates that an excitation-energy distribution of width $\Gamma/1.5$ cannot be formed within a time shorter than $1.5\hbar/\Gamma$. Evidently, one has to abandon the point of view according to which it is sufficient for nuclei to remain "passively" in the excited state within the time $\tau = \hbar/\Gamma$, on average, for the formation of a gamma-ray spectrum with a width Γ. Instead, one has to accept the concept of an excited nucleus as a generator of electromagnetic oscillations that acts within the whole time over which the nucleus remains in the excited state. Below, we will show that there are other physics factors supporting the concept of a protracted character of nuclear radiative processes.

As for our experiments devoted to measuring the magnetic-field- perturbed ADs of resonantly scattered gamma rays of ^{191}Ir, it follows from them that, if the Mössbauer gamma line exciting nuclei has a natural width, the average lifetime of these nuclei in the respective excited state is 1.5 τ, as the theory requires. This means that the transition of the nucleus from the ground to an excited state and the inverse transition last a short time in relation to τ. Thus, we arrive at the conclusion that, although nuclear transitions proceed via photon absorption and emission, the time scales of these transitions and radiative processes are drastically different. At the onset of gamma-wave interaction with a nucleus, the latter goes over quickly to an excited state, acquiring its spin, parity, and magnetic moment, but the energy of this state has a large uncertainty over the initial period of gamma-wave absorption. This is because the excitation-energy distribution at this instant must be determined by the frequency spectrum (Fourier integral) of that part of gamma- radiation wave train which had time to act on the nucleus by this instant. The longer the time within which the wave train acts on the nucleus, the narrower the excitation-energy distribution and, accordingly, the higher the degree to which the energy of the excited state turns out to be determined. The broadness of the excitation-energy distribution within the initial period of the gamma-wave-absorption process must stem from a high probability of photon emission over this period. Owing to this enhancement of the decay, the value 1.5 τ appears instead of the value 2.5 τ required by the Krylov–Fock theorem. It is noteworthy that, according to the Krylov–Fock theorem, the form prescribed by this theorem for the initial excitation-energy distribution remains invariable in the course of time—only its intensity changes. In our model, the form of this distribution must also change: it becomes narrower in the course of the protracted process of gamma-wave interaction with the nucleus.

Under these conditions, the Krylov–Fock theorem cannot describe correctly the process of decay of an excited nuclear state. This theorem is valid in the case where the distribution $W(E_\gamma)$ arises within a time that is much shorter than the characteristic time of decay of the respective excited state; moreover, the form of the distribution arising at the initial instant must not change under any external effects disturbing the nuclei during the decay process. Such conditions arise, for example, in experiments aimed at observing magnetic-field-perturbed ADs of resonantly scattered bremsstrahlung photons that are generated by decelerated electrons. In that case, the wave trains of the radiation to be absorbed are very short, while the photon spectrum is wide; as a result, one can consider this spectrum in the region of the nuclear resonance as an energy-independent constant. As a result, the excitation-energy distribution is described by the Lorentzian function (2.28) and is formed within a time interval short in relation to τ. For this case, expression (1.82) for $\Delta >> \Gamma$ and the Krylov–Fock theorem give identical values, equal to τ, for the average time within which nuclei remain in the excited state.

It is noteworthy that, by definition, the values of t_{av} that are obtained from experiments devoted to measuring magnetic-field-perturbed ADs of resonantly scattered gamma rays and from the Krylov–Fock theorem have the same meaning. In either case, one averages the lifetime of a nucleus over the time dependence of the photon-emission probability. In the first case, one averages the angle of rotation of the AD rosette, $\Delta\theta = \Omega t$ (t is the lifetime of a specific nucleus in the excited state), with respect to its unperturbed position, and this is equivalent to the averaging of t. In the second case, one averages the value of t directly. Naturally, the uncertainty principle plays a decisive role in the nuclear radiative processes being considered: one cannot create the excitation-energy distribution of characteristic width Γ by acting on nuclei within a time shorter than $\hbar/\Gamma$, nor is it possible to obtain a gamma line of width Γ unless each excited nucleus emits a gamma wave train within $\tau = \hbar/\Gamma$, on average.

In connection with the foregoing, we will try to estimate the scale of the uncertainty in the spatial position of a photon. From two well-known relations $\Gamma\tau = \hbar$, and $\Delta p \times \Delta x \sim \hbar$, it follows that $\Gamma\tau \sim \Delta p \times \Delta x$. For the photon, we have $\Delta p = \frac{\Delta E}{c}$, where E is its energy and c is the speed of light. Obviously, the uncertainty ΔE in the photon energy must be set to Γ. We then have $\Gamma\tau \sim \frac{\Gamma}{c} \times \Delta x$ or $\Delta x \sim c\tau$. This means that the uncertainty in the photon coordinate x is on the same order of magnitude as the length of the wave train emitted by the nucleus involved over its average lifetime in the excited state. It is noteworthy that one cannot interpret this estimate of Δx as a consequence of the uncertainty in the photon-emission instant within τ, assuming that this process is short-term. In the above derivation, the instant of the nuclear transition to the excited state was not fixed in any way, so that this instant cannot be used to reckon time from it. Moreover, τ can also be determined experimentally without fixing of this instant, as was done in our experiments discussed above and devoted to studying the magnetic-field-perturbed ADs of resonantly scattered ^{191}Ir gamma rays. Unfortunately there is no until now the explanation why the wave train of a photon lose suddenly wave properties and

behaves as a like point particle, for example in the Compton scattering. Here is an interesting picture of a similar process not giving however its cause and mechanism. Imagine the two-dimensional plane with zero thickness on which the fragment of straight line is moving. Suddenly this fragment turns so that its ends go out in the third dimension. The point is left on the plane—the place of the fragment intersection with it. The "wave" turned into "particle" and this happened during the zero time independently on the speed of the fragment rotation.

We now consider the Fourier frequency spectrum of an extremely short wave train of a photon as yet another argument in favor of the statement that gamma-ray emission and absorption are protracted processes. If one admits, in accordance with Migdal's treatment, that the time of photon emission is $\lambda\!\!\!^{-} / c$, then the length of the corresponding wave train must be about 1/6 of the period *T;* that is, it must have the form $\sin\omega_o t$, where $0 < t < T/2\pi$. Calculating the Fourrier integral for a signal of duration equal to one period of oscillations, we obtain

$$f(\omega) = \frac{1}{2\pi}\int_0^T \sin\omega_0 t\, e^{i\omega t} dt = \frac{1}{2\pi}\int_0^T \frac{e^{i\omega_0 t} - e^{-i\omega_0 t}}{2i} e^{i\omega t} dt = \frac{1}{4\pi i}\int_0^T \left[e^{i(\omega_0+\omega)t} - e^{-i(\omega_0-\omega)t}\right] dt$$
$$= -\frac{1}{4\pi}\left[\frac{e^{2\pi i\frac{\omega}{\omega_0}} - 1}{\omega + \omega_0} + \frac{e^{2\pi i\frac{\omega}{\omega_0}} - 1}{\omega - \omega_0}\right] = \frac{e^{2\pi i\frac{\omega}{\omega_0}} - 1}{2\pi} \times \frac{\omega_0}{\omega^2 - \omega_0^2}. \tag{2.35}$$

The squared modulus of this amplitude is

$$|f(\omega)|^2 = \frac{1}{2\pi^2\omega_0^2}\frac{1}{\left[\left(\frac{\omega}{\omega_0}\right)^2 - 1\right]^2}\left(1 - \cos 2\pi\frac{\omega}{\omega_0}\right) = \frac{\omega_0^2\left(1 - \cos 2\pi\frac{\omega}{\omega_0}\right)}{2\pi^2\left(\omega_0^2 - \omega^2\right)^2}. \tag{2.36}$$

The graph of this function is shown in Fig. 2.18. The width of the resulting frequency spectrum is many times larger than the natural width of nearly any gamma line emitted by excited nuclei. If, for example, one locates the Mössbauer gamma line of ^{57}Fe (14.4 keV) at the point $\omega/\omega_0 = 1$, then its natural width is about 3.3×10^{-13} on the scale of Fig. 2.18.

There may arise the question of whether the manifestation of a spatial and a time extension of photons is due to the possibility of discriminating between photons by their origin. First of all, we note that, in detecting a single photon, one cannot reveal its wave properties. In order to observe the interference and diffraction patterns and to establish the resonant character of photon interaction with nuclei, one has to detect a large number of photons. At the same time, corpuscular properties of a photon such as its momentum and energy and the coordinates of the vertices of its interaction with the detector material can be determined upon detection by the Compton effect or by the photoabsorption of a single photon. It can be stated that photons of different origin cannot be distinguished in processes where their corpuscular properties are revealed. At the same time, photons of different origin are

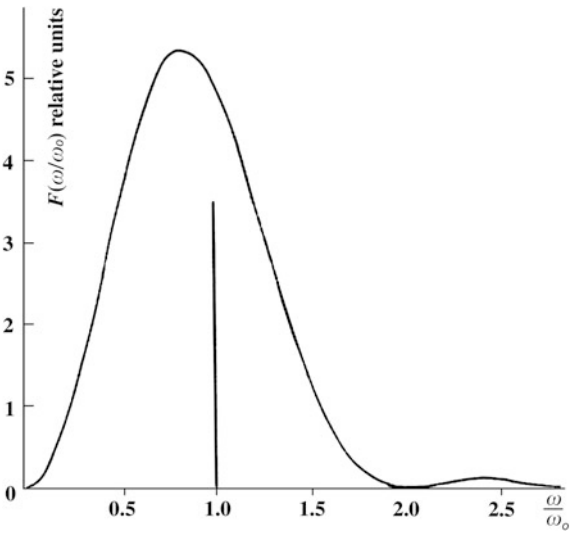

Fig. 2.18 Fourier integral $I_F(\omega)$ for a single period of the sinusoid $\sin(\omega_o t)$. The vertical straight line $\omega/\omega_o = 1$ represents symbolically the Mössbauer gamma line of energy $\hbar\omega_o$. If it was the gamma line of the Mössbauer nuclide ^{57}Fe, then its FWHM value would be about 3.1×10^{-13} on the scale of this figure

distinguishable by their wave properties, but this distinction manifests itself only in an ensemble of photons—one cannot notice them in detecting single photons. For example, electron bremsstrahlung followed by nuclear absorption creates a natural Lorentzian distribution of excitation energies, which leads to a natural average lifetime of nuclei in the excited state and to the exponential decay law. However, the irradiation of the same nuclei with Mössbauer photons resonant for them creates, as was shown above, an excitation-energy distribution that is 1.5 times narrower, which is associated with the corresponding increase in the average lifetime of excited nuclei. We note that the need for detecting many microscopic objects in order to reveal their wave properties permits pinpointing the category (wave versus corpuscular) to which one measured characteristic of a microscopic object or another belongs. For example, the particle spin, which cannot be determined in detecting a single particle, must be classed with wave characteristics of the object. Indeed, it is the spin orientation that determines the particle-beam polarization, which is of course a wave characteristic.

We now revisit expression (1.87), which refers to the case where a nucleus is excited by gamma rays whose spectrum has a characteristic width Δ much smaller than the natural width Γ of the excited nuclear level. Obviously, the average lifetime of excited nuclei emitting such a narrow gamma line (of course, these nuclei are not those that are excited) is Δ/Γ times as long as $\tau = \hbar/\Gamma$. It seems that wave trains corresponding to photons of such a narrow spectrum must act on the nuclei to be excited over the time $\hbar/\Delta >> \hbar/\Gamma$, on average. From Eq. (1.87), it follows, however, that this time does not exceed $2\hbar/\Gamma$, becoming still shorter in the presence of a shift of the exciting gamma line with respect to the absorption line. This means that the excited nucleus terminates the process of resonant interaction with the exciting photon earlier than, as may appear, the completion of the action of a long wave train

on the nucleus must occur. With it all, however, the nucleus absorbs completely the energy of the exciting photon. This is because the energy of a photon is determined by its frequency rather than by the number of oscillations in the corresponding wave train. A mysterious disappearance of the unabsorbed wave-train residue is one of the manifestations of the so-called collapse of the photon wave function—one of the most enigmatic phenomena of quantum physics.

Let us imagine an experiment in which scatterer nuclei are excited by gamma rays of a uniform continuous spectrum. Nuclei excited under these conditions emit photons forming a gamma line of natural width because, in this case, there arises an excitation-energy distribution of the Lorentzian shape, which is natural for the nuclei being considered, so that the decay of excited states will be exponential.

Exponential gamma decay occurs in those cases where the nuclei involved are excited by gamma rays whose wave trains are short and the frequency distributions are wide. This situation may be exemplified by the excitation of nuclei by electron bremsstrahlung, as well as by Coulomb excitation.

Pick out from the excited nuclei ensemble the group of nuclei with exit action energies lying in a narrow area around the energy E_γ. Evidently these nuclei were excited by resonant absorption of gamma rays related to the such narrow area of energy. Therefore the mean life time for nuclei of this group must be determinate be formula (1.87). To obtain the mean life time for total ensemble of excited nuclei one has to average the quantity related to narrow line over the excitation energy *distribution of the ensemble. If this distribution has f Lorentzian shape we obtain*

$$t_{\text{av}} = \frac{\int\limits_{-\infty}^{\infty} \frac{\Gamma^2/4}{\left(E_0-E_\gamma\right)^2+\Gamma^2/4} \times \frac{\Gamma^2/2}{\left(E_0-E_\gamma\right)^2+\Gamma^2/4}\,\tau\,dE_\gamma}{\int\limits_{-\infty}^{\infty} \frac{\Gamma^2/4}{\left(E_0-E_\gamma\right)^2+\Gamma^2/4}\,dE_\gamma} = \tau. \tag{2.37}$$

This means that the energy of a photon plays a significant role in this procedure, but that its frequency spectrum does not affect the result.

In a similar way, one can calculate the average lifetime of excited nuclei for the case of "ideal" Mössbauer resonant gamma-ray scattering as well—that is, for a process in which the emission and absorption lines have the Lorentzian shape with natural width and in which there is no shift between them. In this case, the distribution of excitation energies is determined by the product of two identical

Lorentzian functions. For t_{av}, we then have

$$t_{\text{av}} = \frac{\int\limits_{-\infty}^{\infty} \left[\frac{\Gamma^2/4}{\left(E_0-E_\gamma\right)^2+\Gamma^2/4}\right]^2 \times \frac{\Gamma^2/2}{\left(E_0-E_\gamma\right)^2+\Gamma^2/4}\,\tau\,dE_\gamma}{\int\limits_{-\infty}^{\infty} \left[\frac{\Gamma^2/4}{\left(E_0-E_\gamma\right)^2+\Gamma^2/4}\right]^2 dE_\gamma} = 1.5\tau. \tag{2.38}$$

Thus, a recipe for calculating the average lifetime of nuclei in an excited state have been obtained for the case where the excitation-energy distribution $W(E_\gamma)$ is known. It is the following:

$$t_{\text{av}} = \frac{\int\limits_{-\infty}^{\infty} W(E_\gamma) \times \dfrac{\Gamma^2/2}{(E_0 - E_\gamma)^2 + \Gamma^2/4} \tau \, dE_\gamma}{\int\limits_{-\infty}^{\infty} W(E_\gamma) \, dE_\gamma}. \tag{2.39}$$

Of course, the spectrum of gamma rays emitted by nuclei of a resonant scatterer is identical in all cases to the excitation-energy distribution $W(E_\gamma)$.

References

1. R.F. Metzger, Nucl. Phys. **27**, 612 (1961)
2. A.V. Davydov, V.P. Selyutin, Bull. Acad. Sci. USSR: Phys. **27**, 875 (1963)
3. L.L. Lee, L. Meyer-Schutzmeister, J.P. Schiffer, D. Vincent, Phys. Rev. Lett. **3**, 223 (1959)
4. A. Bussiere de Nercy, M. Langevin, M. Spigel, Comp. Rend. **250**, 1031 (1960)
5. E. Kankeleit, Z. Physik **164**, 442 (1961)
6. O.I. Sumbaev, A.I. Smirnov, V.S. Zykov, Soviet JETP **42**, 115 (1962). (in Russian)
7. *Radionuclide Transformations—Energy and Intensity of Emissions. ICRP Publication 38* (Pergamon Press, Oxford, 1983), ^{182}Ta
8. K.C.J. Goebel, W. McVoy, Phys. Rev. **148**, 1021 (1966)
9. N.A. Voinova, B.S. Dzhelepov, *Isobaric Nuclei with Mass Number A = 182* (Nauka, Leningrad, 1968). (in Russian)
10. M.R. Schmorak, Nucl. Data Sheets **14**, 559 (1975)
11. E.A. Phillips, L.Grodzins, in *Perturbed Angular Correlations,* ed. by E. Karlsson, E. Matthias, K. Siegbahn, (North-Holland Publishing Cmp, Amsterdam, 1964), p, 294
12. D.A. Agresti, E. Kankeleit, B. Persson, Phys. Rev. **155**, 1342 (1967)
13. N. Sikazono, H. Takekoshi, T. Shoji, J. Phys. Soc. Jpn **20**, 271 (1965)
14. S.G. Cohen, N.A. Blum, Y.W. Chow et al., Phys. Rev. Lett. **16**, 322 (1966)
15. R.B. Frankel, Y.W. Chow, L. Grodzins, J. Wulff, Phys. Rev. **186**, 381 (1969)
16. A.V. Davydov and O.N. Sorokin, in *The Results of the Experiment. Adduced in the lecture by A.V. Davydov Resonant Scattering of Gamma Rays*, ed. by A.F. Ioffe, Proceedings of 5-th winter school on nuclear theory and physics of high energy of LPTI, part II, Leningrad (1970), p. 263 (in Russian)
17. J.A. Cameron, L. Keszthelyi, G. Mezei et al., Can. J. Phys. **50**, 736 (1972)
18. Y.W. Chow, L. Grodzins, P. Barrett, Phys. Rev. Lett. **15**, 369 (1965)
19. L. Grodzins, Ann. Rev. Nucl. Sci. **18**, 291 (1968)
20. G. Goldring, R. Kalish, H. Spehl, Nucl. Phys. **80**, 33 (1966)
21. R.L. Mössbauer, Z. Physik **151**, 124 (1958)
22. R.L. Mössbauer, Z. Naturforsch. **14a**, 211 (1959)
23. F. Wittmann, Z. Naturforsch. **19a**, 1409 (1964)
24. G.H.R.Kegel, Thesis MIT. Quoted in [28]
25. H. Korner, J. Radeloff, E. Bodenstedt, Z. Physik **172**, 279 (1963)
26. G. Goldring, Z. Vager, Phys. Rev. **127**, 929 (1962)
27. V.A. Klyucharev, A.K. Valter, I.I. Zalyubovskii, V.D. Afanasiev, Soviet JETP **17**, #3, (1963)

28. R.P. Scharenberg, J.D. Kurfess, G. Schilling et al., Nucl. Phys. **58**, 658 (1964)
29. W. Ebert, O. Klepper, H. Spehl, Nucl. Phys. **73**, 217 (1965)
30. B. Persson, H. Blumberg, D. Agresti, Phys. Rev. **170**, 1066 (1968)
31. I. Ben Zvi, P. Gilad, M.B. Goldberg et al., Nucl. Phys. **A151**, 401 (1970)
32. D.A. Garber, M. Behar, W.M.C. King et al., Phys. Rev. **C9**, 2399 (1974)
33. A.M. Muminov, Abstract of a physics-mathematics candidate dissertation, Tashkent, 1972. (in Russian)
34. A.Z. Dolginov, *Gamma-rays* (Publishing house of Academy of Sciences of USSR, 1961), p. 523 (in Russian)
35. G. Frauenfelder, R. Steffen, Angular Correlations, in *Alfa-, Beta- and Gamma-Ray spectroscopy*, ed. by K. Siegbahn (North-Holland Publishing Company, Amsterdam, 1965). V.2
36. A.V. Davydov, G.R. Kartashov, Y.V. Khrudev, Phys. Nucl. A **7**, 447 (1968)
37. K.S. Krane, At. Data Nucl. Data Tables **# 2**,137 (1976)
38. B.V. Narasimha Rao, S. Jnanananda, Proc. Phys. Soc. **87**, part 2, 455 (1966)
39. E.E. Berlovich, Yu.K. Gusev, V.V. Il'in, M.K. Nikitin, Soviet JETP **43**, 1625 (1962) (in Russian)
40. J. Lindskog, T. Sundström, P. Sparrman, Z. Physik **170**, 347 (1962)
41. S.G. Malmskog, A. Bäcklin, Ark. f. Fysik **39**, 411 (1969)
42. P.P. Craig, J.C. Dash, A.D. McGuire et al., Phys. Rev. Lett. **3**, 221 (1959)
43. P. Steiner, E. Gerdau, W. Hautsch, D. Steenken, Z. Physik **221**, 281 (1969)
44. B. Balko, G.R. Hoy, Phys. Rev. B **10**, 36 (1974)
45. W. Meisel, L. Keszthelyi, Hyperfine Interact. **3**, 413 (1977)
46. M.B. Lewis, Nucl. Data Sheets **9**, 479 (1973)
47. F. Wagner, G. Kaindl, P. Kienle et al., Z. Physik **207**, 500 (1967)
48. S. Gustaffsson, K. Johansson, E. Karlsson et al., Ark. f. Fysik **34**, 169 (1967)
49. F. Wagner, W. Potzel, in *Hyperfine Interactions in Excited Nuclei*, ed. by G. Goldring, R. Kalish, V. II, (Gordon and Breach Science Publishers, New York-London-Paris, 1971), p. 681
50. R.L. Mössbauer, M. Lengsfeld, W. Von Lieres et al., Z. Naturforsch. **26a**, 343 (1971)
51. J.A. Cameron, J.A. Campbell, J.F. Compton et al., Nucl. Phys. **59**, 475 (1964)
52. U. Atzmoni, E.R. Bauminger, D. Lebenbaum et al., Phys. Rev. **163**, 314 (1967)
53. M. Kontani, J. Itoh, J. Phys. Soc. Jpn **22**, 345 (1967)
54. V. Kogan, V.D. Kul'kov, L.P. Nikitin et al. Soviet JETP 18, #2 (1964)
55. W.R. Owens, B.I. Robinson, S. Jha, Phys. Rev. **185**, 1555 (1969)
56. P.C. Riedli, Phys. Rev. B **8**, 5243 (1973)
57. K. Johansson, E. Karlsson, L.O. Norlin, *International Conference on Hyperfine Interactions Studied in Nuclear Reactions and Decay* (Uppsala, Sweden, 1974) (Contributed papers. Upplands Grafiska AB. Uppsala, 1974), p. 164
58. I. Vincze, Solid State Commun. **10**, 341 (1972)
59. A. Narath, Phys. Rev. **165**, 506 (1968)
60. F. Wagner, J. Klöckner, N.J. Körner et al., Phys. Lett. **25B**, 253 (1967)
61. A.V. Davydov, M.M. Korotkov, P.I. Romasheva, JETP Lett. **31**, 560 (1980)
62. A.V. Davydov, M.M. Korotkov, P.I. Romasheva, Bull. Acad. Sci. USSR: Phys **44**, 1 (1980)
63. F.E. Wagner, Hyperfine Interact. **13**, 149 (1983)
64. R. Ehehalt, E. Nolte, F.E.Wagner, H.J. Körner (To be published)
65. V.R. Vanin, N.L. Maidana, R.M. Castro et al., Nucl. Data Sheets **108**, 2393 (2007)
66. G.V. Smirnov, Y.V. Shvyd'ko, Soviet Phys. JETP **68**, 444 (1989)
67. R. Avida, I. Ben Zvi, P. Gilad et al., Nucl. Phys. **A147**, 200 (1970)
68. N.F. Il'khamdzhanov, P.S. Radzhapov, K.T. Salimbaev, Izvestia Acad. Sci. USSR, Ser. Phys. Math. **4**, 79 (1973) (in Russian)
69. K.S. Krane, W.A. Steyert, Phys. Rev. C **9**, 2063 (1974)
70. A. Aharoni, Phys. Rev. B **2**, 3794 (1970)
71. K.S. Krane, B.T. Murdoch, W.A. Steyert, Phys. Rev. Lett. **30**, 321 (1973)
72. P. Raghavan, At. Data Nucl. Data Tables **42**, 189 (1989)

73. W.R. Kölbl, J. Billowes, J. Burde et al., Nucl. Phys. **A456**, 349 (1986)
74. A.E. Stuchbery, S.S. Anderssen, E. Bezakova, Hyperfine Interact. **97/98**, 479 (1996)
75. E. Bezakova, A.E. Stuchbery, H.H. Bolotin et al., Nucl. Phys. **A669**, 241 (2000)
76. A.V. Stepanov, YuM Tsipenyuk, Phys. Usp. **43**, 79 (2000)
77. A.B. Migdal, *Qualitative Methods in Quantum Theory* (W.A. Benjamin Inc, London, Amsterdam, Don Mils. Ontario, Sydney, Tokyo, 1977)
78. N.S. Krylov, V.A. Fock, Soviet JETP **17**, 93 (1947). (in Russian)
79. A.V. Davydov, P.I. Romasheva, Bull. Acad. Sci. USSR: Phys. **45**, 58 (1981)

http://www.springer.com/978-3-319-10523-9

Advances in Gamma Ray Resonant Scattering and Absorption
Long-Lived Isomeric Nuclear States
Davydov, A.V.
2015, XI, 192 p. 71 illus., Hardcover
ISBN: 978-3-319-10523-9